

Maximizing average throughput in oscillatory biological synthesis systems: an optimal control approach

M. Ali Al-Radhawi¹, Michael Margaliot², and Eduardo D. Sontag^{1,3,*}

¹Departments of Bioengineering, and Electrical and Computer Engineering, Northeastern University, Boston MA 02115.

²Department of Electrical Engineering-Systems, Tel Aviv University

³Laboratory of Systems Pharmacology, Program in Therapeutic Science, Harvard Medical School, Boston MA 02115

*Corresponding Author: sontag@sontaglab.org

June 30, 2020

Abstract

A dynamical system *entrains* to a periodic input if its state converges globally to an attractor with the same period. In particular, for a constant input the state converges to a unique equilibrium point for any initial condition. We consider the problem of maximizing a weighted average of the system's output along the periodic attractor. The *gain of entrainment* is the benefit achieved by using a non-constant periodic input relative to a constant input with the same time average. Such a problem amounts to optimal allocation of resources in a periodic manner. We formulate this problem as a periodic optimal control problem which can be analyzed by means of the Pontryagin maximum principle or solved numerically via powerful software packages. We then apply our framework to a class of occupancy models that appear frequently in biological synthesis systems and other applications. We show that, perhaps surprisingly, constant inputs are optimal for various architectures. This suggests that the presence of non-constant periodic signals, which frequently appear in biological occupancy systems, is a signature of an underlying *time-varying* objective functional being optimized.

Keywords: entrainment, contractive systems, systems biology, gene expression, ribosome flow model, optimal control theory.

1 Introduction

Periodic oscillations are abundant in biomolecular systems, and an extensive body of research has been devoted to study their roles in intracellular and extracellular interactions [17, 48]. In the presence of such excitations, proper functioning of biological systems often requires their internal states to *synchronize* with the periodic input signal. In the parlance of systems

theory, this is known as *entrainment*, which means that the response of a system subject to a periodic input with period T will converge to a periodic trajectory of the same period T . There has been great recent interest in the study of this phenomenon [15, 30, 24, 29, 41]. Examples of external periodic influences include operation under the influence of sunlight, which requires the internal clocks of biological organisms to entrain to the 24-hour solar day. For instance, it has been shown that the plant *Arabidopsis* uses its circadian clock to anticipate times with an increased susceptibility to fungal pathogens, and regulates its immune system resources accordingly [22]. Entrainment is also essential in many *synthetic* biological systems. For instance, synthetic oscillators can be used to emulate natural hormone release rhythms in the treatment of certain diseases [25]. More generally, robust and optimal synthetic oscillators constitute an important module in larger systems [37, 21].

At the intracellular level, the *cell cycle* is a periodic routine that regulates DNA replication and cell division. This requires precise regulation of many interacting proteins, and also appropriate resource allocation at different stages of the cell cycle. Deviations from the program can lead to cell death or cancer.

An important underlying process is translation, which is a major component in the central dogma of molecular biology, and requires sophisticated coordination between ribosomes, mRNA and tRNA molecules, and various proteins. Two of the key underlying steps are *initiation* in which the ribosome attaches to an mRNA molecule, and *elongation*, in which the ribosome scans along the mRNA to produce a chain of amino-acids. Regulation of initiation and elongation are an effective way to control protein concentrations [45, 19]. One biological mechanism for cell-cycle regulated genes is based on codons whose corresponding tRNAs have low abundances (known as non-optimal codons) [16, 52]. In particular, *periodic* variations in the level of these specific tRNAs can generate cell cycle-dependent oscillations in the corresponding protein levels [16]. In other words, the protein levels entrain to the periodic excitation provided by the tRNA levels. Similar oscillation-inducing regulation mechanisms during DNA damage response have also been reported [33]. Other works have indicated that the speed of translation is sensitive to fluctuating tRNA availability [49], that cells use tRNA to control protein abundance in stress conditions [47], and that tRNA dysregulation is a contributing factor in cancer progression [20]. In addition to tRNA regulation, many other intracellular oscillators have been identified as regulators of the cell cycle [11, 12].

In what follows, we first describe, as a motivation, a class of mathematical models that are useful in modeling various processes involved in gene translation. Our focus is to analyze these models in the presence of periodic excitations modeled as periodic inputs. We then state the generic control problem to be solved.

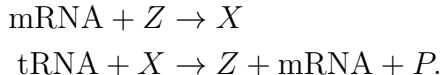
1.1 Motivation: Occupancy models

In many important biological models, state variables describe the occupancy in a certain site or compartment. For example, in physiology compartmental models describe drug absorption distribution and elimination in various body fluids or tissues [3].

One-dimensional models

Many biological processes involve “biological machines” that move along a 1D lattice of ordered “sites”. Examples include ribosomes that scan mRNA during translation, molecular motors that carry cargoes along a filamentous network in the cytoskeleton, and phosphotransferases that transfer the phosphoryl group from the sensor kinases to some ultimate target. To be concrete, we focus on ribosomes and mRNA translation, but the same ideas apply to other models.

We now derive such a 1D occupancy model using several alternative modeling approaches. Let X (Z) be the species denoting bound (unbound) ribosomes, respectively. The free ribosomes bind to mRNA. Bound ribosomes need tRNAs to translate the information in the mRNA into proteins (P). A phenomenological one-step model written in Chemical Reaction Network (CRN) formalism [13] gives:



We assume that tRNA and mRNA are abundant, so that their dynamics are not affected by the above reactions. Note that the species tRNA represents all possible variants of transfer RNA. Let $x(t)$ be the concentration of occupied (bound) ribosomes in the cell at time t , and let $z(t)$ be the concentration of free ribosomes. The occupancy of ribosomes is determined by mRNA transcript abundance $u_0(t)$, and tRNA abundance $u_1(t)$. The CRN gives the following system of bilinear ODEs:

$$\begin{aligned} \dot{x}(t) &= u_0(t)z(t) - u_1(t)x(t), \\ \dot{z}(t) &= u_1(t)x(t) - u_0(t)z(t). \end{aligned} \tag{1}$$

Assuming a fixed total concentration of ribosomes M , we have $x(t) + z(t) \equiv M$. The total concentration can be normalized to $M = 1$. Then the two-dimensional dynamics can be reduced to a one-dimensional ODE:

$$\dot{x}(t) = u_0(t)(1 - x(t)) - u_1(t)x(t). \tag{2}$$

This implies that $x(t)$ evolves on the unit interval, and it can be interpreted as a normalized occupancy of some site at time t . More generally, $x(t)$ can be interpreted as the probability that a certain site is occupied by some “biological machine” like a ribosome or a molecular motor. This occupancy model has been termed a “bottleneck” module in [42].

Note that the occupancy model (1) can also be used to model binding and unbinding of a substrate to an enzyme.

Multisite models: The Ribosome Flow Model

The Totally Asymmetric Simple Exclusion Process (TASEP) [8] is a fundamental stochastic model from nonequilibrium statistical physics. In TASEP, particles move forward at random times along a 1D chain of sites. A site can be either free or contain a single particle. Totally asymmetric means that the flow is unidirectional, and simple exclusion means that a particle can only hop into a free site. This models the fact that two particles cannot be in the same

place at the same time. The simple exclusion paradigm generates an indirect coupling between the particles, and also allows modeling the evolution of “traffic jams”: if a particle remains at site i for a long time, then particles will accumulate “behind” it, i.e. in site $i - 1$, then site $i - 2$ and so on. TASEP has been used extensively to model and analyze ribosome flow [53] and many more natural and artificial processes including molecular motors, traffic flow, evacuation dynamics, and more [44].

The *Ribosome Flow Model* (RFM) [39] is the dynamic mean-field approximation of TASEP. In the RFM, the state-variables $x_1(t), \dots, x_n(t)$ describe the occupancy in n sites along the mRNA molecule. The RFM dynamics is described by a system of n first-order ODEs:

$$\dot{x}_k = \lambda_{k-1}x_{k-1}(1 - x_k) - \lambda_k x_k(1 - x_{k+1}), \quad k = 1, \dots, n, \quad (3)$$

where we define $x_0(t) \equiv 1$ and $x_{n+1}(t) \equiv 0$. Here $x_i(t)$ describes the occupancy at site i at time t , normalized such that $x_i(t) = 0$ [$x_i(t) = 1$] means that site i is completely empty [full] at time t . In the context of translation, $\lambda_i(t) > 0$ describes the transition rate from site i to site $i + 1$ at time t . This rate depends on various biomechanical properties, for example, the abundance of tRNA molecules delivering the amino-acids to the ribosomes. Eq. (3) can be explained as follows. The change in the density in site k is the flow from site $k - 1$ into site k minus the flow from site k to site $k + 1$. The first term, $\lambda_{k-1}x_{k-1}(1 - x_k)$, is proportional to the transition rate from site $k - 1$ to k , the occupancy at site $k - 1$, and the amount of “free space” ($1 - x_k$) at site k . Note that this is a “soft” version of simple exclusion. The second term is similar. Note that $\lambda_n(t)x_n(t)$ describes the flow of ribosomes out of the last site at time t , i.e. the protein production rate. If the whole mRNA strand is considered as one site, that is, $n = 1$ then the RFM model will be identical with the occupancy model (2).

The state-space of the RFM is the n -dimensional unit cube $[0, 1]^n$. It was shown in [31] that the RFM (with constant λ_i 's) admits a unique equilibrium $x_e = x_e(\lambda_0, \dots, \lambda_n) \in (0, 1)^n$, and that for any $a \in [0, 1]^n$ the corresponding solution of (3) satisfies $\lim_{t \rightarrow \infty} x(t; a) = x_e$. In other words, the transition rates determine a unique Globally Asymptotically Stable (GAS) equilibrium. More generally, Ref. [30] showed that if the rates are time-varying, and jointly periodic with a period T , then (3) admits a GAS solution $\gamma_T : \mathbb{R}_+ \rightarrow (0, 1)^n$, that is T -periodic, and $x(t, a)$ converges to γ_T for all $a \in [0, 1]^n$. In other words, the RFM entrains. Note that a constant rate is T -periodic for any T , so entrainment also holds if a single rate is T -periodic and all the other rates are constant. In the biological context, entrainment can be interpreted as follows: if, say, variations in tRNA abundances generate T -periodic initiation and/or elongation rates, then the protein production rate will also converge to a periodic pattern with period T .

The RFM and its variants have been used extensively to model and analyze ribosome flow during the process of translation (see e.g. [32, 50, 38, 35]), as well as other important cellular processes like phosphorelay [4].

Just like TASEP, the RFM (and in particular the model (1)) is a phenomenological model that can be applied to study various processes like vehicular or pedestrian traffic [42]. In this case, the occupancy is interpreted as the ratio between the number of vehicles (or pedestrians) at a certain junction at time t and the total number of possible vehicles.

Generalized occupancy models

Let $\mathbb{R}_+^n := \{x \in \mathbb{R}^n \mid x_i \geq 0, i = 1, \dots, n\}$ denote the non-negative orthant in \mathbb{R}^n . Recall that the linear single-input single-output (SISO) linear system

$$\begin{aligned}\dot{x} &= Ax + bu, \\ y &= c^T x,\end{aligned}$$

is called *positive* if every entry of b, c , and every off-diagonal entry of A is non-negative (that is, A is a *Metzler* matrix). This implies that for any $x(0) \geq 0$ and any control u with $u(t) \geq 0$ for all t we have $x(t) \geq 0$ and $y(t) \geq 0$ for all $t \geq 0$ [14]. This is useful when the state-variables and the output represent physical quantities that can never attain negative values, e.g., population sizes or concentrations of molecules.

Generalized occupancy models (GOMs) are a cascade of occupancy models and SISO positive linear systems. These models are useful when the output of an occupancy model is the input to another biological system, that in the vicinity of its equilibrium point, can be approximated as a positive linear dynamical system. Similar to the multisite RFM model introduced before, it can be shown that GOMs entrain to periodic inputs.

For example, Fig. 1-(a) depicts a time-varying bottleneck module feeding a positive linear system. In this module, u_0, u_1 are entrance rates, and w_1 is the exit rate. The effective inflow is proportional to the *vacancy* $1 - x(t)$, while the outflow is proportional to the *occupancy* $x(t)$. This cascade models an occupancy model driving a downstream linear system. As another example, Fig. 1-(b) depicts a linear system “sandwiched” between a 2-site RFM and 1-site RFM. This can model a situation where the production rate of one protein affects, via another biological process, the promoter (and thus the transcription initiation rate) of some other mRNA.

A GOM can also be used to model the RFM with time-varying rates under the condition

$$\lambda_i(t) \gg \lambda_0(t) \text{ for all } i \geq 1 \text{ and all } t \geq 0. \quad (4)$$

Then we can expect that the initiation rate becomes the bottleneck rate and thus $x_i(t)$, $i = 2, \dots, n$, converge to values that are close to zero, suggesting that (3) can be simplified to

$$\begin{aligned}\dot{x}_1(t) &= \lambda_0(t)(1 - x_1(t)) - \lambda_1(t)x_1(t), \\ \dot{x}_i(t) &= \lambda_{i-1}(t)x_{i-1}(t) - \lambda_i(t)x_i, \quad i \in \{2, \dots, n\},\end{aligned} \quad (5)$$

which has the same form as the cascade in Fig. 1-(a).

After these motivating examples, we next formulate the abstract questions to be studied in this paper.

1.2 Gain of entrainment

Entrainment can be studied in the framework of systems and control theory. The periodic excitation is modeled as the control input $u(t)$ of a dynamical system, and the system entrains if in response to a T -periodic excitation it admits a globally attractive T -periodic solution γ_T . In other words, every solution of the system converges to the attractor γ_T .

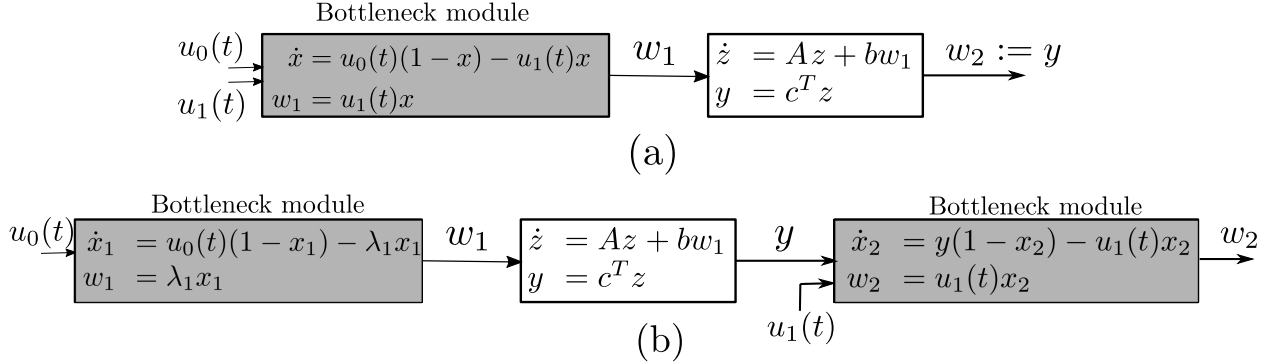


Figure 1: Two examples of generalized occupancy models . The controls are $u_0(t), u_1(t)$ which are scalar functions. We have $x_1, x_2, x, w_1, w_2, y \in \mathbb{R}_+, z \in \mathbb{R}^n, A \in \mathbb{R}^{n \times n}, b, c \in \mathbb{R}_+^n$. The linear system block is assumed to be positive and Hurwitz.

Here, we consider a *quantitative* potential advantage of entrainment called the *gain of entrainment*. To explain this, consider a control system that, for any $T \geq 0$ and any T -periodic control u_T , entrains to a unique T -periodic solution γ_T . Note that, in particular, this implies that for any constant control $u(t) \equiv u_0$ the trajectory converges to a unique equilibrium γ_0 for any initial condition. Suppose also that the system admits a scalar output $y(t) = h(t, x(t), u(t))$ (that is, a function of time, state, and the input), and that h is T -periodic in t , so that the output also entrains. The output represents a quantity that we would like to maximize, e.g. traffic flow or protein production rate.

Since the system entrains, we ignore the transients and consider the problem of maximizing the average of the periodic output, that is, the average over a period of $h(t, \gamma_T, u_T)$. The gain of entrainment is the benefit (if any) in the maximization for a (non-trivial) periodic control over a constant control. A natural example is to analyze the gain in traffic flow for periodically-varying traffic signals over constant signals. However, to make this meaningful, we must add another assumption, namely, that the total time of green lights in both alternatives is equal. Mathematically, this means that we compare the average output for a time-periodic control u_T and a constant control \bar{u} such that the average value of u_T over a period is equal to \bar{u} . If the gain of entrainment is positive then entrainment does not only assist in producing an internal clock that can follow an external periodic excitation, but also yields higher production rates than those obtained by equivalent constant excitations.

The possible advantages of periodic forcing of various production processes are well-known. For example, Ref. [5] states that: “...theoretical and experimental studies have shown that the performance (for instance micro-algae or bio-gas production) of some optimal steady-state continuous bioreactors can be improved by a periodic modulation of an input such as dilution rate or air flow”. Ref. [7] studies a PDE model for harvesting a biological resource and demonstrates the advantages of periodic harvesting over a constant one.

The gain of entrainment was recently introduced in [42]. Entrainment in nonlinear systems is nontrivial to prove. A typical proof is based on contraction theory [41, 30], yet this type of proof provides no information on the attractive periodic solution, except for its period (see [10] for some related considerations). Nevertheless, we show here that determining the gain of entrainment can be cast as an *optimal control problem*. This allows using powerful

theoretical tools, like Pontryagin’s maximum principle [36, 27, 28], as well as numerical methods in studying the gain of entrainment. We demonstrate this by analyzing the gain of entrainment in several examples of occupancy models.

For instance, consider the gain of entertainment for (5). It is natural to speculate that using time-periodic rates $\lambda_i(t)$, that are properly synchronized, yields a positive gain of entertainment with respect to using constant rates (with the same average values). In the context of traffic flow, this is equivalent to the conjecture that properly synchronized periodic traffic lights can improve the overall flow. However, we show that, perhaps surprisingly, for a subclass of these systems the gain of entrainment is zero.

We also consider a problem formalism that allows for time-varying costs of resources, like tRNAs, along the period. These may be produced at different unit costs at different times of the cycle. This modified formulation allows the allocation of resources differently at different times along the cycle. Also, instead of average throughput, a *weighted* average of the product may be more relevant, in the sense that we may need certain enzymes at different times of the day or at different points in the cell cycle. This corresponds to “just-in-time production” [51]. In such cases, we show, not so surprisingly, that time-varying periodic inputs may indeed offer an advantage over constant inputs. This suggests that the presence of non-constant periodic signals, which frequently appear in biological occupancy systems, implies that the system is optimising an underlying *time-varying* objective functional.

Our work is related to results from the field of optimal periodic control (OPC) (see, e.g., [9]). As noted by Gilbert [18], OPC was motivated by the following question: Does time-dependent periodic control yield better process performance than optimal steady-state control? In particular, the recent paper [6] defines a notion called *over-yielding* that is closely related to the gain of entrainment. However, our setting is different, as in OPC periodicity was enforced by restricting attention to controls u guaranteeing that $x(T) = x(0)$. This implies in particular that the initial value $x(0)$ (and thus also general transient behaviors) may have a strong effect on the results. Also, in the typical OPC formulation there is in general no requirement that the averages of the periodic and constant controls are equal.

We study systems that entrain and thus for a T -periodic control the state of the system converges to a unique T -periodic trajectory for *any* initial condition $x(0)$. In other words, we consider the behavior of attractors.

The remainder of this paper is organized as follows. The next section defines the gain of entrainment for a general mathematical model. Section 3 shows how the analysis can be cast as an optimal control problem. Section 4 demonstrates the theory for the two-input bottleneck module. Section 5 proves that for several GOMs, including the ones depicted in Fig. 1, the gain of entrainment is zero. Finally, conclusions and future directions are presented in Section 6. The appendix contains proofs of the results including a detailed analysis characterizing extremals via the Pontryagin Maximum Principle (PMP).

2 Gain of entrainment

We consider a general nonlinear control system:

$$\begin{aligned}\dot{x} &= f(x, u), \\ y &= h(t, x, u),\end{aligned}\tag{6}$$

with f, h locally Lipschitz functions, the state $x(t) \in \mathbb{R}^n$, control (or input) $u(t) \in \mathbb{R}^m$, and scalar output $y(t) \in \mathbb{R}$. We allow h to be time-varying to include the cases in which different weights can be used at different times in the cycle. The set of admissible controls consists of measurable functions taking values in some closed and compact set $U \subset \mathbb{R}^m$. Let $x(t, p, u)$ denote the solution of (6) at time $t \geq 0$ for the initial condition $x(0) = p$ and the control u . We assume throughout that for any $x(0)$ in the state-space and any admissible control, (6) admits a unique solution for all $t \geq 0$.

We say that system (6) *entrains* if in response to any admissible and T -periodic control u_T the system admits a unique T -periodic solution $\gamma_T(t)$ (that depends on u_T), and for any initial condition p the solution $x(t, p, u_T)$ converges to γ_T . This implies in particular that the system “forgets” its initial condition.

To explain the mathematical formulation of the gain of entrainment, fix $q \in \mathbb{R}^m$ with $q_i > 0$ for all i . We would like to consider only inputs whose average over a period is q , and compare their effect to the effect of the constant control $u(t) \equiv q$. However, we allow a slightly more general scenario by fixing a weighting function $\alpha(t) > 0$ such that $\frac{1}{T} \int_0^T \alpha(t) dt = 1$. We then restrict attention to T -periodic controls satisfying the weighted integral constraint:

$$\frac{1}{T} \int_0^T \alpha(t) u(t) dt = q,\tag{7}$$

that is, the α -weighted average of u is q . This can be further generalized by allowing a general measure μ on the interval $[0, T]$ and imposing $\int_{[0, T]} u(t) d\mu = q$. However, we keep the presentation simple by adhering to (7).

Let

$$z(u) := \frac{1}{T} \int_0^T h(t, \gamma_T(t), u(t)) dt,\tag{8}$$

that is, the average value of the output along the globally attractive T -periodic solution (recall that we assume that h is T -periodic in its first variable). If the convergence to γ_T is relatively fast then after a short transient the average output over a period of length T is very close to $z(u)$. In applications in fields like biotechnology and traffic control the average value of the output, and not its specific values at all times, is often the relevant quantity.

The constant control $u(t) \equiv q$, which we simply denote by q , is also T -periodic (for any $T \geq 0$) and satisfies (7). Hence, the corresponding solution converges to a fixed point $e = e(q)$ and

$$\begin{aligned}z(q) &= \frac{1}{T} \int_0^T h(t, e, q) dt \\ &= h(e, q).\end{aligned}$$

The *gain of entrainment* of (6) is defined as

$$c_T(q) := \sup_u z(u) - z(q), \quad (9)$$

where the sup is over all admissible, T -periodic controls that satisfy the constraint (7). Thus, we are always comparing the effect of controls with the same average value. Note that $c_T(q) \geq 0$ for all q . If $c_T(q) > 0$ for some q , then there exists a nontrivial periodic control that yields a higher average output than that obtained for a constant control. If $c_T(q) = 0$, then nontrivial T -periodic controls are “no better” than the simple constant control equal to q .

To gain a wider perspective, consider the case of a SISO asymptotically stable LTI system with input [output] $u(t)$ [$y(t)$] and transfer function $G(s)$. Fix $T > 0$, and consider the T -periodic control

$$u_T(t) := a + b \sin(2\pi t/T),$$

with $a, b \in \mathbb{R}$. Note that $\frac{1}{T} \int_0^T u_T(t) dt = a$. Let $\omega := 2\pi/T$. It is well-known that the output converges to the T -periodic function $y_T(t) := G(0)a + |G(j\omega)|b \sin(\omega t + \angle G(j\omega))$, where $j := \sqrt{-1}$, so $\frac{1}{T} \int_0^T y_T(t) dt = G(0)a$. On the other-hand, for the constant control $u(t) \equiv a$ the output converges to $G(0)a$, which is the same value. Thus, for this input the gain of entrainment is zero. Any T -periodic, measurable, and bounded input can be expressed as a Fourier series in terms of sinusoidal functions, and this implies that for LTI systems the gain of entrainment is always zero.

However, for nonlinear system the gain of entrainment may be positive. The next two examples demonstrate this.

Example 1. *Consider the scalar system:*

$$\begin{aligned} \dot{x}(t) &= 1 - x(t)u(t), \\ y(t) &= x(t). \end{aligned} \quad (10)$$

Fix $T > 0$. For a function $v : \mathbb{R}_+ \rightarrow \mathbb{R}_+$, let $\bar{v} := \frac{1}{T} \int_0^T v(s) ds$. Fix $q > 0$. For the control $u(t) \equiv q$ any solution of (10) converges to the equilibrium q^{-1} . Consider a T -periodic and positive control $u_T(t)$ satisfying $\bar{u}_T = q$, and assume there exists some $\alpha > 0$ such that $u_T(t) \geq \alpha$ for almost all $t \in [0, T]$. Then any matrix measure of the Jacobian of (10) is uniformly less or equal than $-\alpha < 0$. Therefore, the system is contractive and any solution of (10) converges to a unique T -periodic solution $x_T(t)$. Let $\omega := 2\pi/T$. Consider now the specific T -periodic control

$$u_T(t) := 1 + (1/2) \cos(\omega t). \quad (11)$$

Here, $q = \frac{1}{T} \int_0^T u_T(t) dt = 1$. For this input, the corresponding solution of (10) is:

$$x(t) = \exp\left(-t - \frac{\sin(\omega t)}{2\omega}\right) (x(0) + \phi(t)),$$

where $\phi(t) := \int_0^t \exp\left(s + \frac{\sin(\omega s)}{2\omega}\right) ds$. In particular,

$$x(T) = \exp(-T)(x(0) + \phi(T)).$$

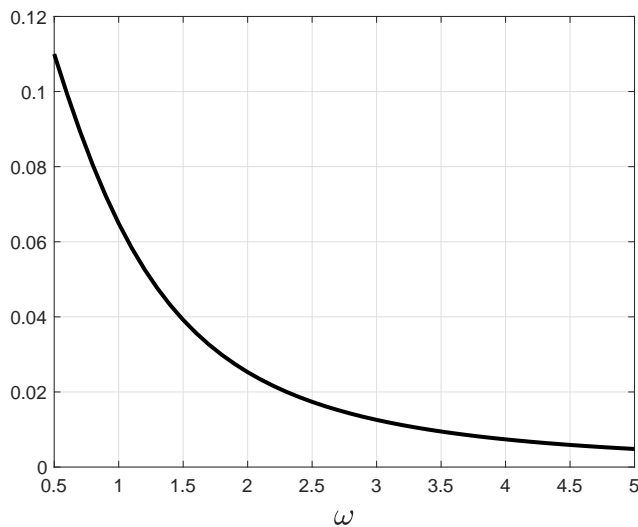


Figure 2: Average value of $x_T(t) - 1$ in Example 1 as a function of $\omega \in [0.5, 5]$.

The initial condition $x(0) = c$ for which the solution is T -periodic is

$$c = \exp(-T)(c + \phi(T)),$$

so

$$c = \frac{\exp(-T)\phi(T)}{1 - \exp(-T)}. \quad (12)$$

Thus, the attractive periodic solution is $x_T(t) := \exp\left(-t - \frac{\sin(\omega t)}{2\omega}\right)(c + \phi(t))$.

The average of the control $u_T(t)$ is $q = 1$. On the other-hand, for the control $u_0(t) \equiv 1$ the solution of (10) converges to the steady-state 1. Fig. 2 depicts the value

$$\frac{1}{T} \int_0^T x_T(t) dt - 1,$$

as a function of $\omega = 2\pi/T$. It may be seen that this is always positive, and is maximal as $T \rightarrow \infty$.

We conclude that for $q = 1$ the gain of entrainment of (10) is positive for any $T > 0$. Note that for large values of ω the gain of entrainment goes to zero. This is expected due to averaging [26]. Roughly speaking, for large values of ω the system cannot track the fast changes in the input, and thus responds to the average of the input. More rigorously, for a system affine in the control, the map from controls on an interval $[0, T]$ to trajectories on $[0, T]$ is continuous with respect to the weak* topology in L^1 and the uniform topology on continuous functions, respectively (see, e.g. [46, Theorem 1]), and (2) for a periodic input $u(t)$, the input $u(\omega t)$ converges weakly to the average of u . An alternative proof is given for example in the textbook [26] (Section 10.2) (changing time scale in the statement of Theorem 10.4, by $x(t) = x(t/\epsilon)$). \square

Example 2. Consider the system:

$$\begin{aligned}\dot{x}_1(t) &= -x_1(t) + u(t), \\ \dot{x}_2(t) &= -x_2(t) + ax_1^2(t), \\ y(t) &= x_2(t),\end{aligned}\tag{13}$$

with $a > 0$.

Consider the input $u_T(t) := 1 + \sin(\omega t)$, with $\omega > 0$. Here, $q = \bar{u} = 1$. Let $T := 2\pi/\omega$, and let $H(s) := \frac{1}{1+s}$. Then x_1 converges to the steady-state solution:

$$x_{1T}(t) := 1 + |H(j\omega)| \sin(\omega t + \angle H(j\omega)).$$

Hence,

$$\begin{aligned}x_{1T}^2(t) &= 1 + 2|H(j\omega)| \sin(\omega t + \angle H(j\omega)) + |H(j\omega)|^2 \sin^2(\omega t + \angle H(j\omega)) \\ &= 1 + \frac{|H(j\omega)|^2}{2} + 2|H(j\omega)| \sin(\omega t + \angle H(j\omega)) - \frac{|H(j\omega)|^2}{2} \cos(2\omega t + 2\angle H(j\omega)).\end{aligned}$$

It follows that x_2 converges to the steady-state solution

$$\begin{aligned}x_{2T}(t) := &a \left(1 + \frac{|H(j\omega)|^2}{2} + 2|H(j\omega)|^2 \sin(\omega t + 2\angle H(j\omega)) \right. \\ &\left. - \frac{|H(j\omega)|^2}{2} |H(2j\omega)| \cos(2\omega t + 2\angle H(j\omega) + \angle H(2j\omega)) \right),\end{aligned}$$

so

$$\bar{x}_{2T} = \frac{1}{T} \int_0^T x_{2T}(t) dt = a \left(1 + \frac{|H(j\omega)|^2}{2} \right).$$

On the other-hand, for the average input $\bar{u} = \frac{1}{T} \int_0^T (1 + \sin(\omega t)) dt = 1$, $x_1(t)$ converges to one, and $x_2(t)$ to a , so the average of the output is a . The difference between the two averaged outputs is thus

$$\frac{a}{2} |H(j\omega)|^2 = \frac{a}{2(1 + \omega^2)}.$$

This is maximized for $\omega = 0$, so the gain of entrainment is at least $c_T(1) = a/2$. Observe that examples with arbitrarily large gain of entrainment can be obtained by taking the constant a in (13) large enough. \square

In the next section, we cast the problem of determining the gain of entrainment as an optimal control problem.

3 Optimal control formulation

Consider the control system (6) with n state-variables and m inputs. We assume that the system entrains. Pick any $T > 0$ and any $q \in \mathbb{R}^m$. We restrict attention to T -periodic controls satisfying the individual weighted average constraints:

$$\frac{1}{T} \int_0^T \Xi(t, u(t)) dt = q,\tag{14}$$

where $\Xi : \mathbb{R}_+^m \times [0, T] \rightarrow \mathbb{R}_+^m$ is an integrable vector positive function that satisfies $\frac{1}{T} \int_0^T \Xi(t, q) dt = q$.

The n -dimensional control system with the integral constraint on the controls (14) can be lifted to an $(n + m)$ -dimensional nonlinear control system by adding m -equations to (6):

$$\dot{\tilde{x}} = \begin{bmatrix} \dot{x} \\ \dot{\xi} \end{bmatrix} = \begin{bmatrix} f(x, u) \\ \Xi(t, u) \end{bmatrix} = F(t, \tilde{x}, u), \quad (15)$$

where $\tilde{x} := [x^T \quad \xi^T]^T$. We impose the boundary conditions:

$$x(0) = x(T), \quad \xi(0) = 0, \quad \xi(T) = Tq. \quad (16)$$

Since we consider systems that entrain, for any T -periodic control there corresponds a unique GAS T -periodic solution $\gamma_T(t)$. The condition $x(0) = x(T)$ guarantees that the maximization is performed over this solution. The other two conditions are equivalent to (14).

To make the problem well-posed, we will assume that controls take values in a hypercube $[\ell, L]^m$ where $0 < \ell < L$. We then formulate an optimal control problem as follows:

Problem 1. Fix values $0 < \ell < q < L$. Find an admissible control u that maximizes the objective functional

$$J(u) := \frac{1}{T} \int_0^T h(t, x(t), u(t)) dt,$$

subject to the ODE (15), the constraint (14), $u_j(t) \in [\ell, L], j = 1, \dots, m, t \in [0, T]$, and the boundary conditions (16).

Note that $J(u)$ is the average value of the output along the globally attractive T -periodic solution (recall that we assume that h is T -periodic in its first variable).

In what follows we always consider systems affine in the control. Then the fact that $[\ell, L]^m$ is compact and convex implies, by Filippov's Theorem (see, e.g. [1]), that the reachable set at any time $t \geq 0$ is compact. Since h is locally Lipschitz, an optimal control exists.

The optimal control formulation allows to apply powerful theoretical tools for solving optimal control problems as well as utilize software packages for numerical solutions (e.g., [34, 40]). In the next section, we demonstrate how to determine the gain of entrainment using this formulation for both time-invariant and time-varying cost functions.

Remark 1. The control signals can be assumed to belong to different intervals. In other words, we can have $u_j(t) \in [\ell_j, L_j], j = 1, \dots, m$. Nevertheless, we have simplified the formulation above by re-scaling the controls so that they all satisfy the same bounds.

The following result is immediate:

Theorem 1. A control u is a solution of Problem 1 iff it maximizes $c_T(u) = z_T(u) - q$ as defined in (9).

In other words, to find the gain of entrainment we must find a control u that solves Problem 1 and then compute $J(u) - q$.

3.1 Pontryagin's Maximum Principle (PMP)

Problem 1 can be studied in the framework of the PMP [36, 27, 28]. The *Hamiltonian* associated with our problem is:

$$\mathcal{H}(t, u, \tilde{x}, p, p_0) := p^T(t)F(t, \tilde{x}, u) + \frac{p_0}{T}h(t, x, u), \quad (17)$$

where $p(t) \in \mathbb{R}^{n+m}$ is the co-state, and the *abnormal multiplier* $p_0 \geq 0$ is a constant.

Proposition 2 (PMP). *Let $u^*(t) \in \mathbb{R}^m, t \geq 0$ be an optimal control for Problem 1, and let $\tilde{x}^* : [0, T] \rightarrow \mathbb{R}^{n+m}$ be the corresponding optimal trajectory. There exist $p_0^* \geq 0$ and $p^* : [0, T] \rightarrow \mathbb{R}^{n+m} \setminus \{0\}$, such that:*

1. *The optimal state $\tilde{x}^*(t)$ and corresponding adjoint $p^*(t)$ satisfy:*

$$\begin{aligned} \dot{\tilde{x}}^* &= \frac{\partial \mathcal{H}}{\partial p}(t, u^*, \tilde{x}^*, p^*, p_0^*), \\ \dot{p}^* &= -\frac{\partial \mathcal{H}}{\partial \tilde{x}}(t, u^*, \tilde{x}^*, p^*, p_0^*). \end{aligned} \quad (18)$$

2. *The control $u^*(t)$ satisfies*

$$\mathcal{H}(t, s, \tilde{x}^*(t), p^*(t), p_0^*) \leq \mathcal{H}(t, u^*(t), \tilde{x}^*(t), p^*(t), p_0^*) \quad (19)$$

for all $s \in [l, L]^m$ and almost every (a.e.) $t \in [0, T]$.

3. *The adjoint satisfies the transversality condition:*

$$p_i^*(0) = p_i^*(T), \quad i = 1, \dots, n. \quad (20)$$

4. *$H(t, u^*(t), \tilde{x}^*(t), p^*(t), p_0^*) = 0$ for all $t \in [0, T]$.*

The proof is given in the Appendix. Utilization of the PMP to deduce the structure of the optimal control is a difficult problem in general. We will show in the next section how it can be utilized in certain cases.

A trajectory $\mathcal{X} := (u(t), \tilde{x}(t), p(t))$ is said to be *feasible* if it satisfies the ODEs (18) and the boundary conditions (16) and (20). A feasible trajectory \mathcal{X} is an *extremal trajectory* if it satisfies the PMP, i.e. if it also satisfies Proposition 2. Observe that any optimal trajectory must be an extremal by Proposition 2.

4 Occupancy models with controlled inflow and outflow

In this section we look more closely at the n -dimensional occupancy model of the form:

$$\begin{bmatrix} \dot{x}_1 \\ \dot{x}_2 \\ \vdots \\ \dot{x}_{n-1} \\ \dot{x}_n \end{bmatrix} = \begin{bmatrix} u_0(t)(1-x_1) - \lambda_1 x_1(1-x_2) \\ \lambda_1 x_1(1-x_2) - \lambda_2 x_2(1-x_3) \\ \vdots \\ \lambda_{n-2} x_{n-2}(1-x_{n-1}) - \lambda_{n-1} x_{n-1}(1-x_n) \\ \lambda_{n-1} x_{n-1}(1-x_n) - u_1(t)x_n \end{bmatrix}. \quad (21)$$

This is an n -dimensional RFM with initiation and exit rates that are non-negative control inputs. Suppose that both $u_0(t), u_1(t)$ are periodic with period $T \geq 0$. It was proved in [30] that the RFM with T -periodic rates entrains, so in particular (21) admits a unique solution $\gamma_T(t)$, with $\gamma_T(0) = \gamma_T(T)$, and $x \rightarrow \gamma_T$ for any initial condition $x(0) \in [0, 1]^n$.

To study the cost of entrainment in this system, fix $0 < \ell < L$. We will assume that the rates $u_0(t), u_1(t)$ are two measurable and essentially locally bounded functions taking values in the interval $[\ell, L]$.

To allow a “fair” comparison between T -periodic controls and constant controls, fix two values $\bar{u}_0, \bar{u}_1 \in (\ell, L)$, and pose integral constraints on the controls:

$$\frac{1}{T} \int_0^T \alpha_0(t) u_0(t) dt = \bar{u}_0, \quad \frac{1}{T} \int_0^T \alpha_1(t) u_1(t) dt = \bar{u}_1, \quad (22)$$

for some given positive measurable functions $\alpha_0(t), \alpha_1(t)$ satisfying

$$\frac{1}{T} \int_0^T \alpha_0(t) dt = \frac{1}{T} \int_0^T \alpha_1(t) dt = 1.$$

We now use Theorem 1 to formulate an optimal control problem that allows finding the gain of entrainment. Introduce the two-dimensional state $\xi := [x_{n+1} \ x_{n+2}]^T$ and let $u := [u_0 \ u_1]^T$. Then the extended system is an $(n+2)$ -dimensional nonlinear control system:

$$\dot{x} := \begin{bmatrix} \dot{x}_1 \\ \dot{x}_2 \\ \vdots \\ \dot{x}_n \\ \dot{x}_{n+1} \\ \dot{x}_{n+2} \end{bmatrix} = f(x) + g(x)u(t), \quad (23)$$

where

$$f(x) := \begin{bmatrix} -\lambda_1 x_1 (1 - x_2) \\ \lambda_1 x_1 (1 - x_2) - \lambda_2 x_2 (1 - x_3) \\ \vdots \\ \lambda_{n-1} x_{n-1} (1 - x_n) \\ 0 \\ 0 \end{bmatrix}, \quad g(x) := \begin{bmatrix} 1 - x_1 & 0 \\ 0 & 0 \\ \vdots & \\ 0 & -x_n \\ \alpha_0(t) & 0 \\ 0 & \alpha_1(t) \end{bmatrix}, \quad (24)$$

and the boundary conditions are:

$$x_i(T) = x_i(0), i = 1, \dots, n, \quad x_{n+1}(0) = 0, \quad x_{n+1}(T) = T\bar{u}_0, \quad x_{n+2}(0) = 0, \quad x_{n+2}(T) = T\bar{u}_1. \quad (25)$$

The optimal control problem is:

Problem 2. Find $u_0, u_1 : [0, T] \rightarrow [\ell, L]$ that maximize the cost functional

$$J(u_0, u_1) := \frac{1}{T} \int_0^T \beta(t) u_1(t) x_n(t) dt, \quad (26)$$

subject to the ODE (23), integral constraints (22), and the boundary conditions (25), where $\beta : [0, T] \rightarrow \mathbb{R}$ is a given non-negative measurable function.

In general, this seems to be a non-trivial problem. Nevertheless, this formulation allows the utilization of both theoretical and numerical optimal control tools, and we will provide exact results in special cases.

4.1 Application of the PMP

As in the previous section, we can write the Hamiltonian (17). In this case,

$$\mathcal{H}(u, x, p, p_0) := p^T(t) (f(x(t)) + g(x(t))u(t)) + \frac{p_0}{T}\beta(t)u_1(t)x_n(t), \quad (27)$$

which can be written as:

$$\mathcal{H} = \varphi_0(t)u_0(t) + \varphi_1(t)u_1(t), \quad (28)$$

where

$$\begin{aligned} \varphi_0(t) &:= p_1(t)(1 - x_1(t)) + \alpha_0(t)p_{n+1}(t), \\ \varphi_1(t) &:= x_n(t)\left(\frac{p_0}{T}\beta(t) - p_n(t)\right) + \alpha_1(t)p_{n+2}(t), \end{aligned} \quad (29)$$

are called the *switching functions*.

4.1.1 Characterization of regular arcs

Let \mathcal{X} be a feasible trajectory. The switching functions φ_0, φ_1 play a special role in determining the optimal control. Define the open set:

$$E_r := \{t \in [0, T] \mid \varphi_0(t)\varphi_1(t) \neq 0\}.$$

A *regular arc* is a restriction $\mathcal{X}|_V$ for some open subset $V \subset E_r$.

Since the Hamiltonian (27) is linear in the control inputs, the optimal control is *bang-bang* when the corresponding switching function does not vanish. This is a well-known result in optimal control. We state it for the sake of completeness.

Lemma 3. *Let \mathcal{X} be an extremal trajectory. Then for any $t \in E_r$ and $i \in \{0, 1\}$ we have*

$$u_i^*(t) = \begin{cases} L, & \text{if } \varphi_i(t) > 0, \\ \ell, & \text{if } \varphi_i(t) < 0. \end{cases}$$

This means that at any time t where $\varphi_i(t) \neq 0$, the corresponding $u_i^(t)$ is a bang-bang control, meaning that it takes extremal values.*

Proof. We prove the result for $i = 0$. (The proof for $i = 1$ is very similar.) Suppose that $\varphi_0(t) > 0$ for some $t \in [0, T]$. Seeking a contradiction, suppose that $u_0^*(t) < L$. Then,

$$\begin{aligned} \mathcal{H}(u_0^*(t), u_1^*(t), x^*(t), p^*(t)) &= \varphi_1(t)u_1^*(t) + \varphi_0(t)u_0^*(t) \\ &< \varphi_1(t)u_1^*(t) + \varphi_0(t)L \\ &= \mathcal{H}(L, u_1^*(t), x^*(t), p^*(t)), \end{aligned}$$

and this contradicts (19). Hence, u_0^* is not optimal. The same argument can be applied when $\varphi_0(t) < 0$. \square

Therefore, unless either of the switching functions vanish on a nonzero measure set, the optimal control is bang-bang, meaning that it has values in $\{\ell, L\}^2$ for almost all t .

4.2 The unweighted optimal control problem

In this section, we consider the unweighted version of Problem 2, that is, the case where $\alpha_0(t) = \alpha_1(t) = \beta(t) \equiv 1$ for all $t \in [0, T]$.

4.2.1 Constant controls satisfy the PMP

We first show that the constant controls satisfy the necessary conditions for optimality.

Theorem 4. *Consider the unweighted Problem 2. The constant controls $u_0(t) \equiv \bar{u}_0$, $u_1(t) \equiv \bar{u}_1$ satisfy Proposition 2 (the PMP) with the corresponding switching functions identically zero.*

Proof. Let $z := [p_1 \ \dots \ p_n]^T$, i.e. the first n entries of the adjoint state. Eq. (18) yields

$$\dot{z} = -J^T(x, u)z - bu_1, \quad (30)$$

where J is the Jacobian of the RFM (21) w.r.t. x , and $b := [0 \ \dots \ 0 \ p_0/T]^T$. Also, $\dot{p}_{n+1}(t) = \dot{p}_{n+2}(t) \equiv 0$.

It has been shown in [31] that the RFM with constant rates admits a unique GAS steady state in $(0, 1)^n$. Hence, every solution of (21) with $u_0(t) \equiv \bar{u}_0$, $u_1(t) \equiv \bar{u}_1$, converges to a point $\bar{x} = [\bar{x}_1 \ \bar{x}_2 \ \dots \ \bar{x}_n]^T \in (0, 1)^n$.

It was shown in [30] that if M is any compact subset of $(0, 1)^n$ then there exists a matrix measure $\mu : \mathbb{R}^{n \times n} \rightarrow \mathbb{R}$ such that $\mu(J(x, u)) < 0$ for all $x \in M, u \geq 0$. This implies in particular that all the eigenvalues of $J(x, u)$ have a negative real part [2], so $J(x, u)$ is nonsingular for each $x \in (0, 1)^n, u \geq 0$. Hence, so is $J^T(\bar{x}, \bar{u})$. Let $\bar{z} := -(J^T(\bar{x}, \bar{u}))^{-1}b\bar{u}_1$. Let $\bar{u} := [\bar{u}_0 \ \bar{u}_1]^T$. We now show that for

$$u(t) \equiv \bar{u}, \ x(t) \equiv \bar{x}, \ p_0 = T, \ p(t) \equiv [\bar{z} \ -\bar{p}_1(1 - \bar{x}_1)/\bar{u}_0 \ -\bar{x}_n(1 - \bar{p}_n)/\bar{u}_1]^T,$$

all the conditions in the PMP hold. First note that the boundary conditions (25) all hold. Eq. (30) holds by the definition of \bar{p} . The switching functions (29) satisfy $\varphi_0(t) \equiv \varphi_1(t) \equiv 0$. Eq. (28) implies that $\mathcal{H} \equiv 0$ and that (19) trivially holds. \square

We have shown that constant controls satisfy the necessary conditions of the PMP. In other words, constant controls are always extremal solutions.

In the next subsection, we show that for $n = 1$ constant controls are the *only* controls that satisfy the PMP.

4.2.2 Extremal analysis of the one-dimensional unweighted problem

In this subsection, we study the following system:

$$\begin{aligned} \dot{x}_1(t) &= u_0(t)(1 - x_1(t)) - u_1(t)x_1(t), \\ \dot{x}_2(t) &= u_0(t), \\ \dot{x}_3(t) &= u_1(t). \end{aligned} \quad (31)$$

The controls u_0 [u_1] represent time-varying initiation [exit] rates in an RFM with $n = 1$. Even though the PMP provides a general approach for addressing optimal control problems, it seldom leads to a full characterization of extremal solutions, especially in the case of multiple inputs. We will show that this is possible for the system (31): a detailed analysis using the PMP shows that any extremal trajectory corresponds to a constant $x_1(t)$. Since each control input takes values in a compact and convex set, the optimal control problem always has a solution. Thus, there is no gain of entrainment. This shows that the PMP is a viable approach for handling such problems and lays the ground for future generalization to higher dimensional cases.

Theorem 5. *Let \mathcal{X} be an extremal trajectory for Problem 2 with the system (31). Then*

$$x_1^*(t) \equiv \frac{\bar{u}_0}{\bar{u}_0 + \bar{u}_1} = \frac{1}{1 + (\bar{u}_1/\bar{u}_0)} \text{ for all } t \in [0, T]. \quad (32)$$

The proof is given in the Appendix.

The PMP immediately yields the following.

Theorem 6. *Fix $0 < \ell < L$, and let the admissible controls u_0, u_1 take values in $[\ell, L]$, with given averages $\bar{u}_0, \bar{u}_1 \in (\ell, L)$, the optimal objective for Problem 2 and system (31) is*

$$J^* = \frac{\bar{u}_0}{\bar{u}_0 + \bar{u}_1}. \quad (33)$$

The optimal trajectory is $x_1^(t) \equiv \bar{u}_0/(\bar{u}_0 + \bar{u}_1)$, a constant, and it can be achieved by the constant inputs:*

$$u_0^*(t) \equiv \bar{u}_0, u_1^*(t) \equiv \bar{u}_1. \quad (34)$$

Remark 2. *The control inputs $u_0(t), u_1(t)$ that achieve the optimal cost are not unique. Indeed, it is clear that the optimal solution in (32) depends only on the ratio \bar{u}_1/\bar{u}_0 . For instance, $u_0^{**}(t) \equiv \bar{u}_0\rho(t), u_1^{**}(t) \equiv \bar{u}_1\rho(t)$ is also an optimal solution for any function ρ such that $\bar{u}_0\rho(t) \subset [\ell, L]$ and $\bar{u}_1\rho(t) \subset [\ell, L]$ for all $t \in [0, T]$.*

Remark 3. *Theorem 6 can be also proven via a more direct approach, motivated by an idea from [23]. This alternative proof is given in the Appendix.*

4.2.3 The unweighted problem for the RFM with $n = 2$ and a single input

We now study Problem 2 for an RFM with $n = 2$ and a single control $u_0(t)$ as the initiation rate, i.e.

$$\begin{aligned} \dot{x}_1 &= u_0(1 - x_1) - \lambda_1 x_1(1 - x_2), \\ \dot{x}_2 &= \lambda_1(1 - x_2)x_1 - \lambda_2 x_2, \\ \dot{x}_3 &= u_0(t), \end{aligned} \quad (35)$$

subject to the boundary conditions (25). Here our goal is to maximize the average value of the output rate $\lambda_2 x_2$.

More formally, we aim at solving the following problem:

Problem 3. Let ℓ, \bar{u}_0, L be given such that $0 < \ell < \bar{u}_0 < L$. Find $u_0 : [0, T] \rightarrow [\ell, L]$ that maximizes the cost functional $J(u_0) := \frac{1}{T} \int_0^T \lambda_2 x_2(t) dt$, that is, the average production rate subject to the ODE (35), integral constraint $\frac{1}{T} \int_0^T u_0(t) = \bar{u}_0$, and the boundary conditions $x_1(0) = x_1(T), x_2(0) = x_2(T)$.

The next result shows that here as well a constant control is optimal, that is, there is no gain of entrainment.

Theorem 7. Fix $0 < \ell < L$ and $\bar{u}_0 \in (\ell, L)$, the objective function for Problem 3 with the system (35) is maximized by the constant control $u_0^*(t) \equiv \bar{u}_0$.

Proof. The first equation in (35) is the first equation (31) for $u_1(t) = \lambda_1(1 - x_2)$, so $\bar{u}_1 = \lambda_1(1 - \bar{x}_2)$, and the output rate is $\lambda_1(1 - x_2)x_1$. (Note that here x_2 is the second state-variable in (35), and not the integral of u_0 as in (31)). By Theorem 6, we have $\lambda_1 \overline{u_1 x_1} \leq (\lambda_1 \bar{u}_1 \bar{u}_0) / (\bar{u}_0 + \lambda_1 \bar{u}_1)$. Hence,

$$\lambda_1 \overline{u_1 x_1} = \lambda_1 \overline{(1 - x_2)x_1} \leq \frac{\lambda_1 \bar{u}_1 \bar{u}_0}{\bar{u}_0 + \lambda_1 \bar{u}_1} = \frac{\lambda_1(1 - \bar{x}_2)\bar{u}_0}{\bar{u}_0 + \lambda_1(1 - \bar{x}_2)}. \quad (36)$$

Integrating (35) we get

$$0 = x_2(T) - x_2(0) = \int_0^T \dot{x}_2(t) dt = \lambda_1 \int_0^T (1 - x_2(t))x_1(t) dt - \int_0^T \lambda_2 x_2(t) dt.$$

Hence, we get that $\lambda_1 \overline{(1 - x_2)x_1} = \lambda_2 \bar{x}_2$. Substituting in (36), we get

$$\lambda_2 \bar{x}_2 \leq \frac{\lambda_1 \bar{u}_0(1 - \bar{x}_2)}{\lambda_1(1 - \bar{x}_2) + \bar{u}_0}. \quad (37)$$

The left-hand side here is the quantity that we are trying to maximize. Rearranging gives:

$$f(\bar{x}_2) \geq 0, \quad (38)$$

where $f(s) := s^2 - \left(1 + \bar{u}_0\left(\frac{1}{\lambda_1} + \frac{1}{\lambda_2}\right)\right)s + \frac{\bar{u}_0}{\lambda_2}$. Let p, q denote the roots of $f(s)$. Then $f(s) = (s - p)(s - q)$ gives

$$\begin{aligned} 1 + \bar{u}_0\left(\frac{1}{\lambda_1} + \frac{1}{\lambda_2}\right) &= p + q, \\ \frac{\bar{u}_0}{\lambda_2} &= pq. \end{aligned} \quad (39)$$

Recall that the RFM (35) with the constant control $u_0(t) \equiv \bar{u}_0$ admits a *unique* steady state $\bar{e} \in (0, 1)^2$ [31]. It is straightforward to show that $f(\bar{e}_2) = 0$. We may assume that $p = \bar{e}_2$, so $p \in (0, 1)$. Then (39) implies that q is real and $q > 1$. The quadratic inequality (38) implies that either $\bar{x}_2 \leq p < 1$ or $\bar{x}_2 \geq q > 1$. Since $x_2(t) \in [0, 1]$ for all t , then the second inequality can be ignored and we have that the maximal (feasible) value of \bar{x}_2 is $\bar{x}_2^* = p = e_2$. Obviously, this is attained for the constant control $u_0(t) \equiv \bar{u}_0$. \square

4.3 Gain of entrainment with time-varying weight functions

Analyzing the case with time-varying weights is challenging, but it is highly relevant to applications since resources may be allocated differently during the period. In this subsection, we show that, even for the above examples, once the weighting functions become time-varying, constant inputs may no longer be optimal.

We consider the special case of (23) with $n = 1$ and a single input $u_0(t)$ as the initiation rate, i.e.

$$\begin{aligned}\dot{x}_1(t) &= u_0(t)(1 - x_1(t)) - \lambda_1 x_1(t), \\ \dot{x}_2(t) &= u_0(t).\end{aligned}\tag{40}$$

Our goal now is to maximize $J(u_0) := \frac{\lambda_1}{T} \int_0^T \beta(t)x_1(t) dt$, subject to the boundary conditions (25), and where the weight function β is differentiable and satisfies $\beta(t) > 0$ for all $t \in [0, T]$. Without loss of generality, we assume that $T = 1$.

Proposition 8. *Suppose that u_0^* is an optimal control. Then for almost all $t \in [0, 1]$ we have that either $u_0^*(t) \in \{\ell, L\}$ or:*

$$u_0^*(t) = c\sqrt{\beta(t)} - \lambda_1 + \frac{\dot{\beta}(t)}{2\beta(t)},\tag{41}$$

for some constant c . Furthermore, if u_0^* satisfies (41) for all $t \in [0, 1]$, then

$$c = \frac{\bar{u}_0 + \lambda_1 - \frac{1}{2} \log \frac{\beta(1)}{\beta(0)}}{\int_0^1 \sqrt{\beta(t)} dt}.\tag{42}$$

Note that if $\bar{u}_0 \in (\ell, L)$ then this implies that the constant control $u_0(t) \equiv \bar{u}_0$ cannot be optimal. If (41) does not hold for any t (e.g. when the right-hand side of (41) takes values that are not in $[\ell, L]$) then the optimal control is bang-bang.

As a specific example take

$$\ell = 0.001, \quad L = 10, \quad \bar{u}_0 = 2, \quad \lambda_1 = 1,$$

and the weight function

$$\beta(t) = e^{-\rho(t-(T/2))^2},$$

with $\rho = 100$ and $T = 1$. In the context of the RFM, this would represent the case where it is required to highly express a specific protein near the middle of every cycle, rather than having a uniform level of production along the entire period.

The constant input $u_0(t) \equiv 2$ yields a steady-state trajectory $x(t) \equiv 2/3$. The corresponding value of the objective function is

$$J(u_0) = \frac{2}{3} \int_0^1 \beta(t) dt = 0.118164.\tag{43}$$

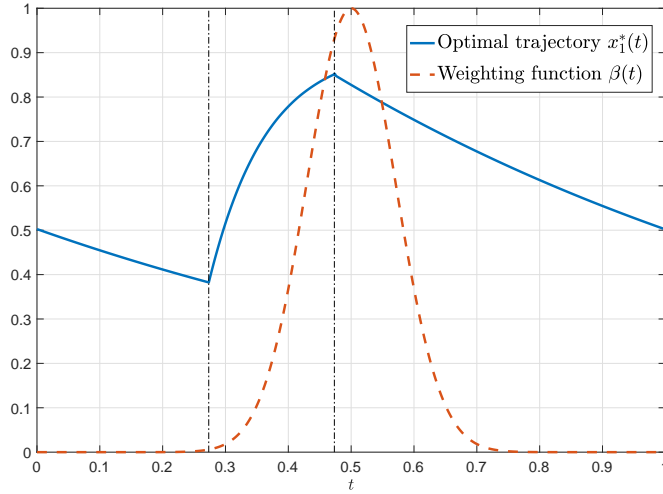


Figure 3: The optimal trajectory for maximizing a weighted throughput is *non-constant*. The plot shows the weighting function $\beta(t)$ with the corresponding optimal periodic solution $x_1^*(t)$. The vertical dashed lines denote the switching points of the three-arc bang-bang controller. Note that the high bang control is switched on when the value of the weight function becomes non-negligible.

Our optimal control formulation can be used to solve the problem *numerically* using optimal control packages like [34]. The result is a three-arc bang-bang control

$$u^*(t) = \begin{cases} \ell, & t \in [0, t_1), \\ L, & t \in [t_1, t_1 + \Delta), \\ \ell, & t \in [t_1 + \Delta, 1], \end{cases}$$

where $\Delta := (\bar{u}_0 - \ell)/(L - \ell) = 0.19992$, and $t_1 = 0.27335$. The corresponding periodic solution satisfies $x(1) = x(0) = 0.50251$. This achieves a cost $J(u^*) = 0.141183$, which is roughly 20% better than (43).

Fig. 3 depicts the approximate optimal bang-bang control (computed using [34] and a bisection procedure) and the resulting periodic solution $x_1^*(t)$. The weight function $\beta(t)$ is also shown. The maximal value of β is achieved at $t = 1/2$. The optimal control switches to the maximal value $L = 10$ before the peak time of β . This makes sense as it guarantees that $x_1^*(t)$ will have large values when the weighting of $x_1^*(t)$ in the cost function is large.

5 Gain of entrainment in generalized occupancy models

In this section, we consider general cascades like those in in Figure 1. Recall that under the conditions (4), the n -dimensional RFM can be approximated by (5), which has the form in Figure 1-(a). We consider here this approximated system.

We first state the following result which is well-known in the theory of linear time-invariant systems (see also [42]). We include the proof for completeness.

Proposition 9. *Consider a single-input-single-output linear system: $\dot{z} = Az + bw$, $y = c^T z$, where $z \in \mathbb{R}^n$, and A is Hurwitz. Let w be a bounded measurable input which is T -periodic. Then y converges to a steady-state T -periodic solution y_w , and*

$$\int_0^T y_w(t) dt = H(0) \int_0^T w(t) dt,$$

where $H(s) := c^T (sI - A)^{-1} b$ is the transfer function of the linear system.

Proof. Since w is measurable and bounded, $w \in L_2([0, T])$. Hence, it can be written as a Fourier series $w(t) = \bar{w} + \sum_i a_i \sin(\omega_i t + \phi_i)$. The output of the linear system converges to the steady-state periodic solution

$$y_w(t) = H(0)\bar{w} + \sum_i |H(j\omega_i)| a_i \sin(\omega_i t + \phi_i + \angle(H(j\omega_i))).$$

Each sinusoid in the expansion has period T , so $\int_0^T y_w(t) dt = TH(0)\bar{w}$. □

Combining Proposition 9 with our results on the gain of entrainment in certain bottleneck models yields the following result.

Theorem 10. *Consider the nonlinear system depicted in either Figure 1-(a) or Figure 1-(b) with A Metzler, and $b, c \in \mathbb{R}_+^n$. Let $u_0(t), u_1(t)$ be T -periodic non-negative control signals. For any $0 < \ell < L$ and any $\bar{u}_0, \bar{u}_1 \in (\ell, L)$, consider the functional*

$$J(u_0, u_1) := \frac{1}{T} \int_0^T w_2(t) dt,$$

where $w_2(t)$ is the steady-state T -periodic output signal. Then the constant controls:

$$u_0^*(t) \equiv \bar{u}_0, \quad u_1^*(t) \equiv \bar{u}_1. \tag{44}$$

maximize J .

Proof. Consider the system depicted in Figure 1-(a). Fix admissible T -periodic controls $u_0(t), u_1(t)$. Denote the corresponding steady-state average values of $w_1(t)$ and $y(t)$ by \bar{w}_1 and \bar{y} . Obviously, $\bar{w}_2 = \bar{y}$. By Proposition 9, $\bar{w}_2 = H(0)\bar{w}_1$, where H is the transfer function of the linear system. Since A is Metzler and $b, c \in \mathbb{R}_+^n$, the trajectories of the linear system are positive. Thus, maximizing J is equivalent to maximizing \bar{w}_1 . Theorem 6 implies that the constant controls $u_0^*(t) \equiv \bar{u}_0$ and $u_1^*(t) \equiv \bar{u}_1$ maximize \bar{w}_1 . The system in Figure 1-(b) can be treated similarly. □

Remark 4. *The same result holds if the single-input modules in Figure 1 are replaced by the single-input RFM with $n = 2$ in (35) as shown in Figure 4.*

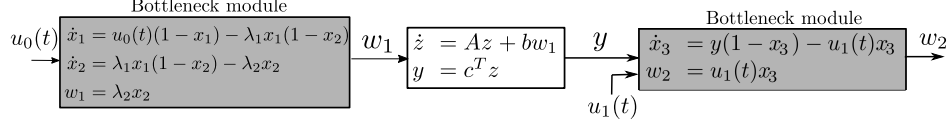


Figure 4: A generalized occupancy model with a 2D bottleneck entrance. The controls are $u_0(t), u_1(t)$ which are scalar functions. We have $x_1, x_2, x_3, w_1, w_2, y \in \mathbb{R}_+, z \in \mathbb{R}^n, A \in \mathbb{R}^{n \times n}, b, c \in \mathbb{R}_+^n$. The linear system block is assumed to be positive and Hurwitz.

6 Discussion

Entrainment is an interesting and important property of dynamical systems. It allows systems to develop an “internal clock” that synchronizes to periodic excitations like the 24h solar day. Such clocks are important in biology, as they allow organisms to adequately respond to periodic processes like the solar day and the cell cycle division process. They are also essential for synthetic biology, as a common clock is an important ingredient in building synthetic biology circuits that include several modules working in synchrony.

Here, we considered an additional qualitative property called the *gain of entrainment*. This measures the advantage, if any, of using a periodic control vs. an “equivalent” constant control for maximizing the average throughput. We showed how this problem can be cast as an optimal control problem. This allows using the sophisticated analytical and numerical tools developed for solving optimal control problems to determine the gain of entrainment.

We have shown that, perhaps surprisingly, there is no gain of entrainment in a class of systems relevant to biology and traffic applications. In other words, in these systems non-constant periodic controls are no better than constant controls. The optimality of constant controls fails to hold if we allow *time-varying* objective functionals. Hence, this suggests the possibility that the observation of non-constant periodic signals in biological systems is correlated with the maximization of the throughput with varying weights along each period or cycle.

An interesting research direction is to generalize these results to models such as the nonlinear n site RFM with $(n + 1)$ time-periodic control inputs.

Appendix: Additional Proofs

A.1 Proof of Proposition 2

Most of the statements here are the standard PMP. We only need to prove the transversality condition (20).

Pick a set $S \subseteq \mathbb{R}^{2(n+m)}$, and suppose that the state must satisfy the constraint $[x(0)^T \ x(T)^T]^T \in S$. Then the corresponding transversality condition [27] is

$$\begin{bmatrix} p(0) \\ -p(T) \end{bmatrix} \perp \mathcal{T}_{\begin{bmatrix} x(0) \\ x(T) \end{bmatrix}} S,$$

where $\mathcal{T}_z S$ denotes the tangent space of S at z . In our case, (16) gives

$$S = \{z \in \mathbb{R}^{2n+2m} \mid [z_1, \dots, z_n]^T = [z_{n+m+1}, \dots, z_{2n+m}]^T, [z_{n+1}, \dots, z_{n+2}]^T = 0, [z_{2n+m+1}, \dots, z_{2n+2m}]^T = Tq\}.$$

Hence, $T_z S = \text{span}\{v^1, \dots, v^n\}$, where v^i is the vector with one at entries i and $(i + n + m)$, and zero elsewhere. Therefore, it is necessary that $p_i^*(0) = p_i^*(T)$, $i = 1, \dots, n$. \blacksquare

A.2 Proof of Theorem 5

The proof, based on the analysis of extremals, is divided into a sequence of Lemmas. For a set $A \subset \mathbb{R}$, $\mu(A)$ denotes its Lebesgue measure. The set of accumulation points of A is denoted by A' . For $x \in \mathbb{R}$, $\{x\} + A := \{x + a \mid a \in A\}$.

Recall that we consider (31), so

$$\mathcal{H} = p_1(u_0(1 - x_1) - u_1x_1) + p_2u_0 + p_3u_1 + \frac{p_0}{T}u_1x_1.$$

Lemma 11. *The adjoint variables p_i^* satisfy:*

$$\begin{aligned} \dot{p}_1^*(t) &= -(u_0(t) + u_1(t))p_1^*(t) - u_1(t), \\ p_2^*(t) &\equiv p_2^*(0), \\ p_3^*(t) &\equiv p_3^*(0), \end{aligned} \tag{45}$$

with the boundary condition $p_1^*(0) = p_1^*(T)$.

Proof. We first show that we can take $p_0^* = T$. Assume that $p_0^* = 0$. Then (18) yields $\dot{p}_1^* = (u_0^*(t) + u_1^*(t))p_1^*$. Integrating over $[0, T]$, we get

$$\log |p_1^*(T)| - \log |p_1^*(0)| = \int_0^T (u_0^*(t) + u_1^*(t)) dt = T(\bar{u}_0 + \bar{u}_1).$$

By the transversality condition, we know that $p_1^*(0) = p_1^*(T)$, which implies that $\bar{u}_0 + \bar{u}_1 = 0$. This is a contradiction, so we conclude that $p_0^* > 0$, and by scaling the objective function we may take $p_0^* = T$. Now (45) follows from calculating the partial derivatives in (18). \square

Analysis of the switching functions

Using Lemma 11, the switching functions in our case are:

$$\varphi_0(t) = p_1(t)(1 - x_1(t)) + p_2(0), \tag{46}$$

$$\varphi_1(t) = x_1(t)(1 - p_1(t)) + p_3(0). \tag{47}$$

Given an extremal trajectory \mathcal{X} , let

$$E_+^i := \{t \in [0, T] \mid \varphi_i(t) > 0\},$$

$$E_-^i := \{t \in [0, T] \mid \varphi_i(t) < 0\},$$

$$E_0^i := \{t \in [0, T] \mid \varphi_i(t) = 0\},$$

where $i = 0, 1$. Note that E_+^i, E_-^i , $i = 0, 1$, are open relative to $[0, T]$, and $E_0^i, i = 0, 1$, are closed. In particular, all these sets are Lebesgue measurable.

A calculation gives

$$\dot{\varphi}_0(t) = u_1(t)(p_1(t) - (1 - x_1(t))), \tag{48}$$

$$\dot{\varphi}_1(t) = u_0(t)(1 - x_1(t) - p_1(t)). \tag{49}$$

Remark 5. The functions φ_0, φ_1 are absolutely continuous. Hence, they are differentiable almost everywhere and have bounded derivatives. This implies that both φ_0, φ_1 are Lipschitz continuous. Also, since the controls are positive, (48),(49) imply that $\text{sgn}(\dot{\varphi}_0(t)) = -\text{sgn}(\dot{\varphi}_1(t))$ whenever φ_0, φ_1 are both differentiable.

Characterization of singular arcs

In this subsection, we are interested in the case where $\mu(E_0^i) > 0$ for either $i = 0$ or $i = 1$. Let

$$E_s := \{t \in [0, T] \mid \varphi_0(t)\varphi_1(t) = 0\} = E_0^0 \cup E_0^1.$$

Let \mathcal{X} be an extremal trajectory. We call any restriction of \mathcal{X} to any nonzero-measure subset of E_s a *singular arc*.

The following Lemmas characterize the behavior on singular arcs.

Lemma 12. Let \mathcal{X} be an extremal trajectory, and assume that $\mu(E_0^i) > 0$ for some $i \in \{0, 1\}$. Then there exists $c_i \in (0, 1)$ such that

$$x_1^*(t) = c_i \text{ for almost all } t \in E_0^i.$$

Furthermore, $x_1^*(t) = 0$ for almost all $t \in E_0^i$ and the two inputs satisfy:

$$\left(\frac{1}{c_i} - 1\right) u_0^*(t) = u_1^*(t), \text{ for almost all } t \in E_0^i. \quad (50)$$

Proof. Let $E_0^{i'} \subseteq E_0^i$ denote the set of accumulation points of E_0^i . Note that $\mu(E_0^{i'}) = \mu(E_0^i)$, since $E_0^i \setminus E_0^{i'}$ is the set of isolated points of E_0^i which is countable, and hence has measure zero. Let $F_i := \{t \in [0, T] \mid \dot{\varphi}_i^*(t) \text{ exists}\} \cap E_0^{i'}$. Then $\mu(F_i) = \mu(E_0^i)$ since φ_i^* is differentiable a.e.

Fix $t \in F_i$. By definition we have $\varphi_i^*(t) = 0$. We show that $\dot{\varphi}_i^*(t) = 0$ as well. Since t is an accumulation point, $\exists \{t_k\}_{k=1}^\infty \subset E_0^i$ such that $t_k \rightarrow t$. Since φ_i^* is differentiable at t , $\dot{\varphi}_i^*(t) = \lim_{k \rightarrow \infty} (\varphi_i^*(t_k) - \varphi_i^*(t)) / (t_k - t) = 0$. We consider the case $i = 0$ (the proof when $i = 1$ is very similar). Using (46) and (48) the equations $\varphi_0^*(t) = \dot{\varphi}_0^*(t) = 0$ yield $p_1^*(t)(1 - x_1^*(t)) = -p_2^*(0)$, and $p_1^*(t) = 1 - x_1^*(t)$. Since $x_1^*(t) \in (0, 1)$, $p_2^*(0) < 0$ and

$$x_1^*(t) = 1 - p_1^*(t) = c_0, \text{ for all } t \in F_0. \quad (51)$$

where $c_0 := 1 - \sqrt{-p_2^*(0)}$.

Let F_0' be the set of accumulation points of F_0 . Then $\mu(F_0') = \mu(F_0)$. Fix $t \in F_0'$. Hence $\exists \{t_k\}_{k=1}^\infty \subset F_0$ such that $t_k \rightarrow t$. Since $x_1^*(t_k) = c_0$ for all k , $x_1^*(t) = c_0$. Substituting this in (31) proves (50). \square

The next result shows that if an extremal trajectory \mathcal{X} has x_1^* identically constant, then it satisfies (32), and \mathcal{X} consists entirely of singular arcs.

Lemma 13. Let \mathcal{X} be an extremal trajectory. If $x_1^*(t)$ is identically constant on $[0, T]$, then

$$x_1^*(t) \equiv \bar{u}_0 / (\bar{u}_1 + \bar{u}_0). \quad (52)$$

Furthermore, $\varphi_0^*(t)\varphi_1^*(t) \equiv 0$, i.e. $E_s = [0, T]$.

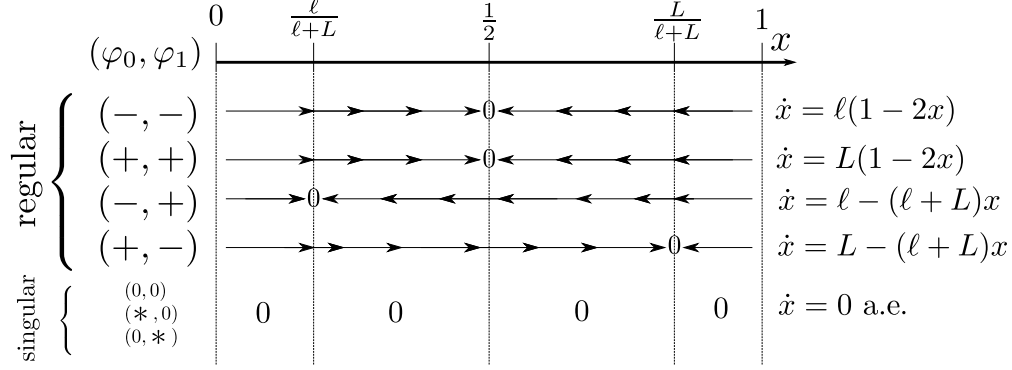


Figure 5: The equation for \dot{x} and the directions of the dynamics as a function of $x \in (0, 1)$ for all possible arcs in an extremal trajectory (see Lemmas 3 and 12). A circle on an axis describes an equilibrium point of the dynamics. The same diagram holds for p , but with all the arrow directions reversed.

Proof. By assumption, there exists $c \in (0, 1)$ such that $c \equiv x_1^*(t)$. Substituting this in (23) yields $\dot{x}_1^* = u_0^*(t) - (u_1^*(t) + u_0^*(t))c \equiv 0$, and integrating over $[0, T]$ proves (52). We also find that $u_1^*(t) \equiv (\frac{1}{c} - 1)u_0^*(t)$, and substituting this in (45) gives $\dot{p}_1^*(t) = u_1^*(t)(-1 - \frac{1}{1-c}p_1^*(t))$. Combining this with the boundary condition (20) gives $p_1^*(t) \equiv c - 1$. Eqs. (46) and (47) give

$$\begin{aligned}\phi_0(t) &= (c - 1)(1 - c) + p_2^*(0), \\ \phi_1(t) &= c(-c) + p_3^*(0),\end{aligned}\tag{53}$$

for all $t \in [0, T]$.

To prove that $E_r = \emptyset$, we first assume that $\mu(E_s) = 0$. Then $E_r = [0, T]$ (a.e.), and Eq. (53) implies that both switching functions are constant and not zero, by the definition of E_r . Lemma 3 implies that every u_i^* is constant, i.e., either $u_i^*(t) \equiv \ell$ or $u_i^*(t) \equiv L$. This contradicts the fact that $\bar{u}_i^* = \frac{1}{T} \int_0^T u_i^*(s) ds \in (\ell, L)$. Thus, $E_s = [0, T]$. We conclude that $\mu(E_s) > 0$. Pick $\tau \in E_s$. Then $\phi_0(\tau) = \phi_1(\tau) = 0$ and (53) implies that $\phi_0(t) = \phi_1(t) = 0$ for all t , so $E_s = [0, T]$. \square

Inadmissibility of Regular Arcs

In the previous subsection we decomposed an extremal trajectory into regular and singular arcs. On the regular arcs, the control is bang-bang. On the singular arcs, the controls satisfy (50) and the state must be constant almost everywhere, so $\dot{x}_1^*(t) = 0$ a.e. In general, an extremal trajectory can consist of an arbitrary patching of regular and singular arcs. In this section, we consider the admissibility of regular arcs.

To simplify presentation, we write x and p instead of x_1 and p_1 from here on. Furthermore, we denote extremal trajectories by x^*, p^* . Figure 5 depicts the dynamics of x based on Lemmas 3 and 12.

Lemma 14. *Let \mathcal{X} be an extremal trajectory. Then $x(t), p(t) \in (\frac{\ell}{L+\ell}, \frac{L}{L+\ell})$ for all $t \in [0, T]$.*

Proof. If $x(t)$ is identically constant then the proof follows from Lemma 13. Hence, we assume that $x(t)$ is not constant. This implies that we can restrict attention to the four regular cases depicted in Figure 5.

Suppose that $x(0) > \frac{L}{L+\ell}$. Then considering the regular cases depicted in Figure 5, we see that $x(T) < \frac{L}{L+\ell}$ and this contradicts the periodicity condition $x(0) = x(T)$.

Suppose that $x(0) = \frac{L}{L+\ell}$. Then considering the regular cases depicted in Figure 5, we see that again $x(T) < \frac{L}{L+\ell}$, as $x(t)$ can increase towards $\frac{L}{L+\ell}$ only in the fourth case depicted in Figure 5, yet it can never reach $\frac{L}{L+\ell}$, as this is an equilibrium (and thus an invariant set) of this dynamics.

Summarizing, we showed that $x(0) > \frac{\ell}{L+\ell}$. Using a similar argument shows that $x(0) \in (\frac{\ell}{L+\ell}, \frac{L}{L+\ell})$, and this implies that $x(t) \in (\frac{\ell}{L+\ell}, \frac{L}{L+\ell})$ for all $t \in [0, T]$. Similar arguments can be used to prove the corresponding statement for p . \square

The following lemma excludes certain transitions between arcs.

Lemma 15. *Let \mathcal{X} be an extremal trajectory. If there exists $\tau \in [0, T]$ such that $\varphi_0(\tau)\varphi_1(\tau) < 0$, then $\varphi_0(t)\varphi_1(t) < 0$ for all $t \in [\tau, T]$.*

Proof. W.l.o.g, assume that $\varphi_0(\tau) < 0$ and $\varphi_1(\tau) > 0$. Hence, $\tau \in E_-^0 \cap E_+^1$. Since both sets are open, there exists a connected component $\mathcal{T} \subset E_-^0 \cap E_+^1$ such that $\tau \in \mathcal{T}$. Let $\mathcal{T}_0, \mathcal{T}_1$ be the connected components containing τ with respect to E_-^0, E_+^1 , respectively. Then $\mathcal{T} = \mathcal{T}_0 \cap \mathcal{T}_1$. Let $\tau_i, i = 1, \dots, 4$, be such that $\mathcal{T}_1 = (\tau_1, \tau_3), \mathcal{T}_0 = (\tau_2, \tau_4)$. W.l.o.g, assume that $\tau_1 \leq \tau_2$.

Assume first that $\tau_2 > 0$. Then there are three possibilities: $\tau_3 < \tau_4, \tau_3 > \tau_4$, and $\tau_3 = \tau_4$; see Figure 6. By definition, $\varphi_0(\tau_2) = 0, \varphi_1(\tau_2) > 0$. Lemma 3 implies that $u_0(t) = \ell, u_1(t) = L$ for all $t \in \mathcal{T}$. By (48) and (49), both φ_0 and φ_1 are differentiable on \mathcal{T} , and the right-derivative $D_{\tau_2^+}^+ \varphi_0$ exists. Since $\varphi_0(\tau_2) = 0$ and $\varphi_0(t) < 0$ on $t \in \mathcal{T}$, we have

$$\begin{aligned} 0 &\geq D_{\tau_2^+}^+ \varphi_0 \\ &= u_1(\tau_2^+)(p(\tau_2) - (1 - x(\tau_2))) \\ &= L(p(\tau_2) + x(\tau_2) - 1). \end{aligned} \tag{54}$$

Recall that $\dot{x}(t) = \ell - (\ell + L)x(t), \dot{p} = (\ell + L)p(t) - L$ for $t \in \mathcal{T}$ (see Figure 5), so

$$\begin{aligned} x(t) &= \left(x(\tau_2) - \frac{\ell}{\ell + L} \right) e^{-(\ell+L)(t-\tau_2)} + \frac{\ell}{\ell + L} \\ &< \left(x(\tau_2) - \frac{\ell}{\ell + L} \right) e^{(\ell+L)(t-\tau_2)} + \frac{\ell}{\ell + L}, \\ p(t) &= \left(p(\tau_2) - \frac{L}{\ell + L} \right) e^{(\ell+L)(t-\tau_2)} + \frac{L}{\ell + L}, \end{aligned} \tag{55}$$

where the inequality (55) follows from the fact that $x(t) > \frac{\ell}{\ell+L}$ (see Lemma 14). Summing up these equations gives

$$x(t) + p(t) < (x(\tau_2) + p(\tau_2) - 1)e^{(\ell+L)(t-\tau_2)} + 1.$$

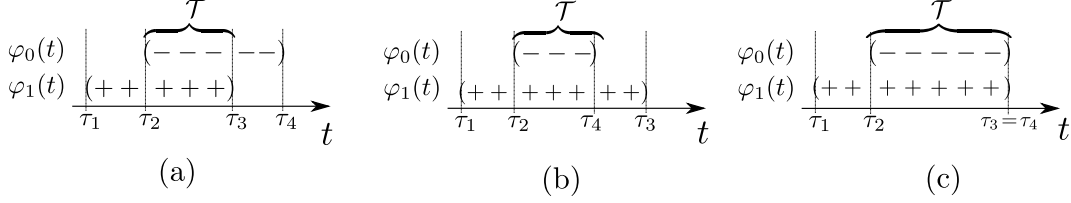


Figure 6: An illustration of the three cases studied in the proof of Lemma 15: (a) $\tau_3 < \tau_4$, (b) $\tau_3 > \tau_4$, (c) $\tau_3 = \tau_4$.

Thus, for any $t \in \mathcal{T}$,

$$\begin{aligned} \dot{\varphi}_0(t) &= L(p(t) + x(t) - 1) \\ &< L(x(\tau_2) + p(\tau_2) - 1)e^{(\ell+L)(t-\tau_2)} \\ &\leq 0, \end{aligned}$$

where the last inequality follows from (54). Hence, $\dot{\varphi}_0(t) < 0$ on \mathcal{T} . Since $\text{sgn } \dot{\varphi}_1(t) = -\text{sgn } \dot{\varphi}_0(t)$, $\dot{\varphi}_1(t) > 0$ for all $t \in \mathcal{T}$.

We now show that $\tau_3 = \tau_4$. Assume that $\tau_3 < \tau_4$. Then $\varphi_0(\tau_3) < 0$ and $\varphi_1(\tau_3) = 0$ as shown in Figure 6(a). Integrating $\dot{\varphi}_1$ over \mathcal{T} , and since $\varphi_1(\tau_2) \geq 0$, we get that $\varphi_1(\tau_3) > 0$, which is a contradiction. Similarly, assuming that $\tau_3 > \tau_4$ gives $\varphi_0(\tau_4) = 0$ (see Figure 6(b)). Since $\varphi_1(\tau_2) = 0$ and $\dot{\varphi}_0(t) < 0$ on \mathcal{T} then $\varphi_0(\tau_4) < 0$, which is a contradiction. Thus, $\tau_3 = \tau_4$ (see Figure 6(c)).

Let $\tau_e := \tau_3 = \tau_4$. Then the preceding argument shows that $\varphi_0(\tau_e) < 0$ and $\varphi_1(\tau_e) > 0$. If $\tau_e < T$ then the definition of τ_3, τ_4 implies that $\phi_0(\tau_e)\phi_1(\tau_e) = 0$. We conclude that $\tau_e = T$. i.e. $\sup \mathcal{T} = T$.

Assume now that $\inf \mathcal{T} = 0$. Since \mathcal{X} is periodic, we can study it on the interval $[0, 2T]$. Let $\tilde{E}_-^0 := E_-^0 \cup (\{T\} + E_-^0)$, $\tilde{E}_+^1 := E_+^1 \cup (\{T\} + E_+^1)$. Hence, define $\tilde{\mathcal{T}}$ as the maximal open neighborhood containing $\tau = T$ in $\tilde{E}_-^0 \cap \tilde{E}_+^1$. The sets $\tilde{\mathcal{T}}_1, \tilde{\mathcal{T}}_2$ are defined similarly. Replicating the previous arguments to the sets $\tilde{\mathcal{T}}, \tilde{\mathcal{T}}_1, \tilde{\mathcal{T}}_2$ we see that $\sup \tilde{\mathcal{T}} = 2T$. Hence, by periodicity, $\sup \mathcal{T} = T$. \square

We can strengthen Lemma 15 to exclude mixed-sign arcs.

Lemma 16. *Let \mathcal{X} be an extremal trajectory. Then, $\varphi_0(t)\varphi_1(t) \geq 0$ for all $t \in [0, T]$.*

Proof. Assume that there exists $\tau \in [0, T]$ such that $\varphi_0(\tau)\varphi_1(\tau) < 0$. Lemma 15 implies that $\varphi_0(t)\varphi_1(t) < 0$ for all $t \in [\tau, T]$. By periodicity, $\varphi_0(0)\varphi_1(0) < 0$. Applying Lemma 15 gives $\varphi_0(t)\varphi_1(t) < 0$ for all $t \in [0, T]$. This implies that both $\varphi_0(t), \varphi_1(t)$ have constant and opposite signs. W.l.o.g, assume that $\varphi_0(t) < 0$ and $\varphi_1(t) > 0$ for all $t \in [0, T]$. By Lemma 3, $u_0(t) \equiv \ell$ and $u_1(t) \equiv L$. Hence, $\dot{x}(t) = \ell - (\ell + L)x(t)$ for all $t \in [0, T]$, so

$$x(T) - x(0) = \left(\frac{\ell}{\ell + L} - x(0) \right) (1 - e^{-(\ell+L)T}).$$

Since $x(0) > \frac{\ell}{\ell+L}$ (see Lemma 14), $x(T) < x(0)$, and this is a contradiction. \square

For an extremal trajectory \mathcal{X} , recall that $E_r := \{t \in [0, T] \mid \varphi_0(t)\varphi_1(t) \neq 0\}$. Lemma 16 implies that

$$E_r = E_{++} \cup E_{--}, \quad (56)$$

where

$$E_{++} := E_+^0 \cap E_+^1 \text{ and } E_{--} := E_-^0 \cap E_-^1.$$

In other words, the only possible bang arcs are the first two cases in Figure 5. Note that $1/2$ is an equilibrium point of both these arcs. Also, on a singular arc $x(t)$ is constant. This proves the following.

Lemma 17. *Let \mathcal{X} be an extremal trajectory. If $x(\tau) \neq 1/2$ for some $\tau \in [0, T]$, then $x(t) \neq 1/2$ for all $t \in [0, T]$*

The next lemma shows that an extremal trajectory must consist of a single singular arc.

Lemma 18. *Let \mathcal{X} be an extremal trajectory. Then, $\varphi_0(t)\varphi_1(t) = 0$ for all $t \in [0, T]$. Furthermore, $x(t) \equiv x(0)$ for all $t \in [0, T]$.*

Proof. We consider two cases.

Case 1. Suppose that there exists a $\tau \in [0, T]$ such that $x(\tau) \neq 1/2$. We may assume w.l.o.g. that $x(\tau) > 1/2$. By Lemma 17, $x(t) > 1/2$ for all $t \in [0, T]$. Seeking a contradiction, assume that $\mu(E_r) > 0$. Then (56) implies that $\dot{x}(t) < 0$ for all $t \in E_r$ (see Figure 5). By Lemma 12, $\dot{x}(t) = 0$ for almost all $t \in E_s$. We conclude that $x(T) < x(0)$, and this is a contradiction. Thus, $\mu(E_r) = 0$.

Case 2. Suppose that $x(t) \equiv 1/2$. Then Lemma 13 implies that $\mu(E_r) = 0$. □

We can now prove Theorem 5. We already know that \mathcal{X} consists of a single singular arc. Lemma 12 implies that there exists a $c \in (0, 1)$ such that $x(t) \equiv c$ for all $t \in [0, T]$. Integrating (50) over $[0, T]$ yields $(\frac{1}{c} - 1)\bar{u}_0 = \bar{u}_1$, and this completes the proof.

A.3 An alternative proof of Theorem 6

The alternative proof is inspired by the completing the square idea in [23] which was used to prove the result for a system with a controlled inflow and a constant outflow (proposed earlier by the authors in the preprint [43]). We show that a similar and simpler approach can be developed to tackle the more general case when both the inflow and outflow can be controlled independently of each other. The proof is based on two Lemmas. Let $T > 0$. Recall that we use the notation $\bar{y} := \frac{1}{T} \int_0^T y(s) ds$.

Lemma 19. *Let $x_1(t)$ be a solution of (31) satisfying $x_1(T) = x_1(0)$. Then $\overline{u_0 x_1^k} = (u_0 + u_1)x_1^{k+1}$ for any integer $k \geq 0$.*

Proof. Since $x_1^{k+1}(T) - x_1^{k+1}(0) = 0$, the integral of

$$\frac{1}{k+1} \frac{dx_1^{k+1}}{dt} = x_1^k \frac{dx_1}{dt} = x_1^k (u_0(1-x_1) - u_1 x_1)$$

is zero, and the result follows. □

For $k = 0, 1$, Lemma 19 gives

$$\begin{aligned}\bar{u}_0 &= \overline{(u_0 + u_1)x_1}, \\ \overline{u_0x_1} &= \overline{(u_0 + u_1)x_1^2},\end{aligned}\tag{57}$$

respectively.

Lemma 20. *Let $x_1(t)$ be a solution of (31) satisfying $x_1(T) = x_1(0)$. Then*

$$\overline{u_1x_1} \leq z,\tag{58}$$

where $z := \bar{u}_0\bar{u}_1/(\bar{u}_1 + \bar{u}_0)$.

Proof. Writing $\overline{u_1x_1} = \overline{((u_0 + u_1) - u_0)x_1}$, and using (57) gives $\overline{u_1x_1} = \bar{u}_0 - \overline{u_0x_1} = \bar{u}_0 - \overline{(u_0 + u_1)x_1^2}$. To apply a completion of squares argument, write this as $\overline{u_1x_1} = z + \frac{\bar{u}_0\bar{u}_0}{\bar{u}_0 + \bar{u}_1} - \overline{(u_0 + u_1)x_1^2}$. Now (57) gives

$$\begin{aligned}\overline{u_1x_1} &= z - \left(\frac{\bar{u}_0\bar{u}_0}{\bar{u}_0 + \bar{u}_1} - \frac{2\bar{u}_0}{\bar{u}_0 + \bar{u}_1} \overline{(u_0 + u_1)x_1} + \overline{(u_0 + u_1)x_1^2} \right) \\ &= z - (u_0 + u_1) \left(x_1 - \frac{\bar{u}_0}{\bar{u}_0 + \bar{u}_1} \right)^2,\end{aligned}$$

and this completes the proof. \square

Eq. (58) implies that $x_1(t) \equiv \frac{\bar{u}_0}{\bar{u}_1 + \bar{u}_0}$ is an optimal trajectory, thus providing an alternative proof to Theorem 5.

A.4 Proof of Proposition 8

The Hamiltonian is $\mathcal{H} = p_1(u_0(1 - x_1) - \lambda_1x_1) + p_2u_0 + \beta(t)\lambda_1x_1$, where we assume w.l.o.g. that $p_0 = T$. Hence, (18) gives

$$\begin{aligned}\dot{p}_1(t) &= (u_0(t) + \lambda_1)p_1(t) - \lambda_1\beta(t), \\ \dot{p}_2(t) &\equiv 0.\end{aligned}$$

The switching function is

$$\varphi_0 = p_1(1 - x_1) + p_2(0),\tag{59}$$

and thus

$$\begin{aligned}\dot{\varphi}_0 &= \lambda_1(p_1 - \beta + \beta x_1), \\ \ddot{\varphi}_0 &= \lambda_1((u_0 + \lambda_1)p_1 - \lambda_1\beta - \dot{\beta} + \dot{\beta}x_1 + \beta(u_0(1 - x_1) - \lambda_1x_1)),\end{aligned}\tag{60}$$

By Lemma 3, an optimal control is bang-bang on E_r . Hence, we study the control on the set $E_0 := \{t \mid \varphi_0(t) = 0\}$ which we assume to have nonzero measure. As in the proof of

Lemma 12, we can find a set $F \subseteq E_0$ such that $F = E_0$ a.e. and $\varphi(t) = \dot{\varphi}(t) = \ddot{\varphi}(t)$ for all $t \in F$. This gives

$$\begin{aligned} p_1(t) &= \beta(t)(1 - x_1(t)), \\ (1 - x(t))^2 &= -p_2(0)/\beta(t), \\ u_0(t) &= \frac{\lambda_1}{1 - x(t)} - \lambda_1 + \frac{\dot{\beta}(t)}{2\beta(t)}, \end{aligned} \tag{61}$$

and this proves (41). Note that this implies that $p_2(0) < 0$. Furthermore, if $E_0 = [0, 1]$, then the equation $\int_0^1 u_0(t) dt = \bar{u}_0$ yields (42).

Acknowledgments

This research has been supported in part by research grants from the Israel Science Foundation, the US-Israel Binational Science Foundation, and NSF 1817936. The authors thank Mahdiar Sadeghi for helpful discussions.

References

- [1] A. A. Agrachev and Y. L. Sachkov, *Control Theory From The Geometric Viewpoint*, ser. Encyclopedia of Mathematical Sciences. Springer-Verlag, 2004, vol. 87.
- [2] Z. Aminzare and E. D. Sontag, “Contraction methods for nonlinear systems: A brief introduction and some open problems,” in *Proc. 53rd IEEE Conf. on Decision and Control*, Los Angeles, CA, 2014, pp. 3835–3847.
- [3] A. J. Atkinson, Jr., “Physiological spaces and multicompartmental pharmacokinetic models,” *Transl. Clin Pharmacol.*, vol. 23, no. 2, pp. 38–41, 2015.
- [4] E. Bar-Shalom, A. Ovseevich, and M. Margaliot, “Ribosome flow model with different site sizes,” *SIAM J. Applied Dynamical Systems*, vol. 19, no. 1, pp. 541–576, 2020.
- [5] T. Bayen, F. Mairet, and M. Sebba, “Study of a controlled Kolmogorov periodic equation connected to the optimization of periodic bioprocess,” *Research Report: INRIA Sophia Antipolis*, 2013.
- [6] T. Bayen, A. Rapaport, and F.-Z. Tani, “Optimal periodic control for scalar dynamics under integral constraint on the input,” *Mathematical Control and Related Fields*, 2019. [Online]. Available: <https://www.aimsociences.org/article/doi/10.3934/mcrf.2020010>
- [7] A. O. Belyakov and V. M. Veliov, “Constant versus periodic fishing: Age structured optimal control approach,” *Math. Model. Nat. Phenom.*, vol. 9, no. 4, pp. 20–37, 2014. [Online]. Available: <https://doi.org/10.1051/mmnp/20149403>
- [8] R. A. Blythe and M. R. Evans, “Nonequilibrium steady states of matrix-product form: a solver’s guide,” *J. Phys. A: Math. Theor.*, vol. 40, no. 46, pp. R333–R441, 2007.

- [9] F. Colonijs, *Optimal Periodic Control*, ser. Lecture Notes in Mathematics. Berlin: Springer-Verlag, 1988, vol. 1313.
- [10] S. Coogan and M. Margaliot, “Approximating the steady-state periodic solutions of contractive systems,” *IEEE Trans. Automat. Control*, vol. 64, no. 2, pp. 847–853, 2018.
- [11] F. R. Cross, “Two redundant oscillatory mechanisms in the yeast cell cycle,” *Developmental Cell*, vol. 4, no. 5, pp. 741–752, 2003.
- [12] J. da Veiga Moreira, S. Peres, J.-M. Steyaert, E. Bigan, L. Paulevé, M. L. Nogueira, and L. Schwartz, “Cell cycle progression is regulated by intertwined redox oscillators,” *Theoretical Biology and Medical Modelling*, vol. 12, no. 1, p. 10, 2015.
- [13] P. Érdi and J. Tóth, *Mathematical Models of Chemical Reactions: Theory and Applications of Deterministic and Stochastic Models*. Manchester University Press, 1989.
- [14] L. Farina and S. Rinaldi, *Positive Linear Systems: Theory and Applications*. John Wiley, 2000.
- [15] J. E. Ferrell Jr, T. Y.-C. Tsai, and Q. Yang, “Modeling the cell cycle: why do certain circuits oscillate?” *Cell*, vol. 144, no. 6, pp. 874–885, 2011.
- [16] M. Frenkel-Morgenstern, T. Danon, T. Christian, T. Igarashi, L. Cohen, Y.-M. Hou, and L. J. Jensen, “Genes adopt non-optimal codon usage to generate cell cycle-dependent oscillations in protein levels,” *Molecular systems biology*, vol. 8, no. 1, 2012.
- [17] E. Fung, W. W. Wong, J. K. Suen, T. Bulter, S.-g. Lee, and J. C. Liao, “A synthetic gene–metabolic oscillator,” *Nature*, vol. 435, no. 7038, pp. 118–122, 2005.
- [18] E. Gilbert, “Optimal periodic control: A general theory of necessary conditions,” *SIAM J. Control Optim.*, vol. 15, no. 5, pp. 717–746, 1977.
- [19] C. Gobet and F. Naef, “Ribosome profiling and dynamic regulation of translation in mammals,” *Current opinion in genetics & development*, vol. 43, pp. 120–127, 2017.
- [20] H. Goodarzi, H. C. Nguyen, S. Zhang, B. D. Dill, H. Molina, and S. F. Tavazoie, “Modulated expression of specific tRNAs drives gene expression and cancer progression,” *Cell*, vol. 165, no. 6, pp. 1416–1427, 2016.
- [21] Y. Guan, Z. Li, S. Wang, P. M. Barnes, X. Liu, H. Xu, M. Jin, A. P. Liu, and Q. Yang, “A robust and tunable mitotic oscillator in artificial cells,” *Elife*, vol. 7, p. e33549, 2018.
- [22] R. A. Ingle, C. Stoker, W. Stone, N. Adams, R. Smith, M. Grant, I. Carre, L. C. Roden, and K. J. Denby, “Jasmonate signalling drives time-of-day differences in susceptibility of Arabidopsis to the fungal pathogen *Botrytis cinerea*,” *The Plant Journal*, vol. 84, no. 5, pp. 937–948, 2015.
- [23] G. Katriel, “Optimality of constant arrival rate for a linear system with a bottleneck entrance,” *Systems & Control Letters*, vol. 138, p. 104649, 2020.

- [24] R. Katz, M. Margaliot, and E. Fridman, “Entrainment to subharmonic trajectories in oscillatory discrete-time systems,” *Automatica*, vol. 116, p. 108919, 2020.
- [25] A. S. Khalil and J. J. Collins, “Synthetic biology: applications come of age,” *Nature Reviews Genetics*, vol. 11, no. 5, pp. 367–379, 2010.
- [26] H. K. Khalil, *Nonlinear Systems*, 3rd ed. Prentice-Hall, 2002.
- [27] E. B. Lee and L. Markus, *Foundations of Optimal Control Theory*. Wiley, 1967.
- [28] D. Liberzon, *Calculus of Variations and Optimal Control Theory: A Concise Introduction*. Princeton University Press, 2011.
- [29] M. Margaliot, L. Grune, and T. Kriecherbauer, “Entrainment in the master equation,” *Royal Society open science*, vol. 5, no. 4, p. 172157, 2018.
- [30] M. Margaliot, E. D. Sontag, and T. Tuller, “Entrainment to periodic initiation and transition rates in a computational model for gene translation,” *PloS one*, vol. 9, no. 5, p. e96039, 2014.
- [31] M. Margaliot and T. Tuller, “Stability analysis of the ribosome flow model,” *IEEE/ACM Transactions on Computational Biology and Bioinformatics (TCBB)*, vol. 9, no. 5, pp. 1545–1552, 2012.
- [32] I. Nanikashvili, Y. Zarai, A. Ovseevich, T. Tuller, and M. Margaliot, “Networks of ribosome flow models for modeling and analyzing intracellular traffic,” *Sci. Rep.*, vol. 9, no. 1, 2019.
- [33] A. Patil, M. Dyavaiah, F. Joseph, J. P. Rooney, C. T. Chan, P. C. Dedon, and T. J. Begley, “Increased tRNA modification and gene-specific codon usage regulate cell cycle progression during the DNA damage response,” *Cell cycle*, vol. 11, no. 19, pp. 3656–3665, 2012.
- [34] M. A. Patterson and A. V. Rao, “GPOPS-II: A MATLAB software for solving multiple-phase optimal control problems using hp-adaptive Gaussian quadrature collocation methods and sparse nonlinear programming,” *ACM Trans. Mathematical Software*, vol. 41, no. 1, pp. 1:1–1:37, 2014.
- [35] G. Poker, Y. Zarai, M. Margaliot, and T. Tuller, “Maximizing protein translation rate in the nonhomogeneous ribosome flow model: A convex optimization approach,” *J. Royal Society Interface*, vol. 11, no. 100, p. 20140713, 2014.
- [36] L. S. Pontryagin, *Mathematical Theory of Optimal Processes*. Routledge, 1962.
- [37] L. Potvin-Trottier, N. D. Lord, G. Vinnicombe, and J. Paulsson, “Synchronous long-term oscillations in a synthetic gene circuit,” *Nature*, vol. 538, no. 7626, pp. 514–517, 2016.
- [38] A. Raveh, M. Margaliot, E. Sontag, and T. Tuller, “A model for competition for ribosomes in the cell,” *J. Royal Society Interface*, vol. 13, no. 116, p. 20151062, 2016.

- [39] S. Reuveni, I. Meilijson, M. Kupiec, E. Ruppin, and T. Tuller, “Genome-scale analysis of translation elongation with a ribosome flow model,” *PLOS Computational Biology*, vol. 7, no. 9, p. e1002127, 2011.
- [40] M. Rieck, M. Bittner, B. Gruter, J. Diepolder, and P. Piprek, “Falcon.m User Guide,” *Institute of Flight System Dynamics, Technical University of Munich*, 2020. [Online]. Available: <https://www.fsd.lrg.tum.de/software/falcon-m/>
- [41] G. Russo, M. di Bernardo, and E. D. Sontag, “Global entrainment of transcriptional systems to periodic inputs,” *PLOS Computational Biology*, vol. 6, no. 4, pp. 1–26, 04 2010. [Online]. Available: <https://doi.org/10.1371/journal.pcbi.1000739>
- [42] M. Sadeghi, M. A. Al-Radhawi, M. Margaliot, and E. D. Sontag, “No switching policy is optimal for a positive linear system with a bottleneck entrance,” *IEEE Control Systems Letters*, vol. 3, no. 4, pp. 889–894, 2019.
- [43] M. Sadeghi, M. A. Al-Radhawi, M. Margaliot, and E. Sontag, “On the periodic gain of the ribosome flow model,” *bioRxiv*, 2018. [Online]. Available: <https://www.biorxiv.org/content/early/2018/12/28/507988>
- [44] A. Schadschneider, D. Chowdhury, and K. Nishinari, *Stochastic Transport in Complex Systems: From Molecules to Vehicles*. Elsevier, 2011.
- [45] N. Sonenberg and A. G. Hinnebusch, “Regulation of translation initiation in eukaryotes: mechanisms and biological targets,” *Cell*, vol. 136, no. 4, pp. 731–745, 2009.
- [46] E. D. Sontag, *Mathematical Control Theory: Deterministic Finite Dimensional Systems*, 2nd ed. New York: Springer, 1998.
- [47] M. Torrent, G. Chalancon, N. S. de Groot, A. Wuster, and M. Madan Babu, “Cells alter their tRNA abundance to selectively regulate protein synthesis during stress conditions,” *Science Signaling*, vol. 11, no. 546, 2018.
- [48] B. P. Tu and S. L. McKnight, “Metabolic cycles as an underlying basis of biological oscillations,” *Nature Reviews Molecular Cell Biology*, vol. 7, no. 9, pp. 696–701, 2006.
- [49] S. E. Wohlgemuth, T. E. Goroehowski, and J. A. Roubos, “Translational sensitivity of the Escherichia coli genome to fluctuating tRNA availability,” *Nucleic acids research*, vol. 41, no. 17, pp. 8021–8033, 2013.
- [50] Y. Zarai, A. Ovseevich, and M. Margaliot, “Optimal translation along a circular mRNA,” *Sci. Rep.*, vol. 7, no. 1, p. 9464, 2017.
- [51] A. Zaslaver, A. E. Mayo, R. Rosenberg, P. Bashkin, H. Sberro, M. Tsalyuk, M. G. Surette, and U. Alon, “Just-in-time transcription program in metabolic pathways,” *Nature Genetics*, vol. 36, no. 5, pp. 486–491, 2004.
- [52] M. Zhou, J. Guo, J. Cha, M. Chae, S. Chen, J. M. Barral, M. S. Sachs, and Y. Liu, “Non-optimal codon usage affects expression, structure and function of clock protein FRQ,” *Nature*, vol. 495, no. 7439, pp. 111–115, 2013.

- [53] R. K. P. Zia, J. Dong, and B. Schmittmann, “Modeling translation in protein synthesis with TASEP: A tutorial and recent developments,” *J. Statistical Physics*, vol. 144, pp. 405–428, 2011.